Journal of the Mechanics and Physics of Solids 139 (2020) 103926

Contents lists available at ScienceDirect

Journal of the Mechanics and Physics of Solids

journal homepage: www.elsevier.com/locate/jmps

Theoretical development of continuum dislocation dynamics for finite-deformation crystal plasticity at the mesoscale

Kyle Starkey[a], Grethe Winther[b], Anter El-Azab[a,*]

[a] School of Materials Engineering, Purdue University, West Lafayette, IN 47907, USA
[b] Department of Mechanical Engineering, Technical University of Denmark, DK-2800 Kgs. Lyngby, Denmark

ARTICLE INFO

Article history:
Received 27 July 2019
Revised 16 February 2020
Accepted 20 February 2020
Available online 5 March 2020

Keywords:
Crystal plasticity
Dislocation dynamics
Dislocation transport

ABSTRACT

The equations of dislocation transport at finite crystal deformation were developed, with a special emphasis on a vector density representation of dislocations. A companion thermodynamic analysis yielded a generalized expression for the driving force of dislocations that depend on Mandel (Cauchy) stress in the reference (spatial) configurations and the contribution of the dislocation core energy to the free energy of the crystal. Our formulation relied on several dislocation density tensor measures linked to the incompatibility of the plastic distortion in the crystal. While previous works develop such tensors starting from the multiplicative decomposition of the deformation gradient, we developed the tensor measures of the dislocation density and the dislocation flux from the additive decomposition of the displacement gradient and the crystal velocity fields. The two-point dislocation density measures defined by the referential curl of the plastic distortion and the spatial curl of the inverse elastic distortion and the associate dislocation currents were found to be more useful in deriving the referential and spatial forms of the transport equations for the vector density of dislocations. A few test problems showing the effect of finite deformation on the static dislocation fields are presented, with a particular attention to lattice rotation. The framework developed provides the theoretical basis for investigating crystal plasticity and dislocation patterning at the mesoscale, and it bears the potential for realistic comparison with experiments upon numerical solution.

1. Introduction

A theoretical development of continuum dislocation dynamics for finite-deformation mesoscale crystal plasticity is presented in this communication. This development is motivated by the progress made in modeling crystal deformation at the mesoscale using dislocation dynamics, with both discrete (Arsenlis et al., 2007; Devincre et al., 2011; Po et al., 2014; Sills et al., 2016; Weygand et al., 2002) and continuum (El-Azab and Po, 2018) representations of the dislocations. This progress showed that a direct coupling of the dislocation theory and continuum mechanics of crystals to study metal plasticity is feasible. Now, an important goal is to extend the dislocation dynamics approach to model finite crystal deformation, which can help us understand the collective dislocation mechanisms of plasticity at experimentally relevant plastic strains. Above few to several percent strain, dislocations self-organize in patterns that influence the flow strength of crys-

* Corresponding author.
E-mail addresses: starkeyk@purdue.edu (K. Starkey), grwi@mek.dtu.dk (G. Winther), aelazab@purdue.edu (A. El-Azab).

https://doi.org/10.1016/j.jmps.2020.103926
0022-5096/

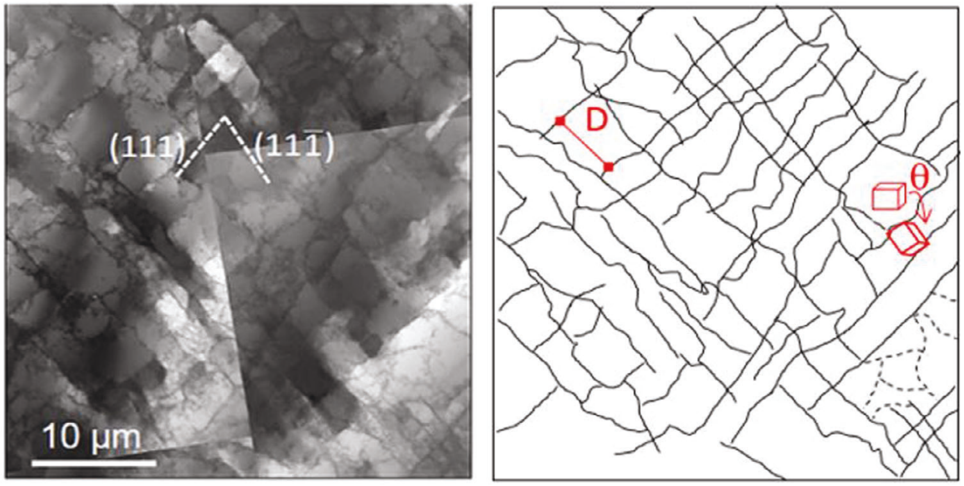

Fig. 1. A TEM micrograph showing a typical dislocation microstructure in rolled aluminum (adopted from Hong et al., 2013) and a tracing of the extended planar boundaries aligned with {111} slip planes (continuous lines) and cell boundaries (dashed lines) . These boundaries are characterized by lattice misorientation and separation distance that were extensively studied (Hughes and Hansen, 2003).

tals. Such patterns are associated with significant lattice misorientation across dislocation walls or boundaries of various types (Hughes et al., 1997).

Continuum dislocation dynamics represent dislocations by density fields governed by transport equations that are solved concurrently with crystal mechanics. Some models within this framework that use a tensor representation of the dislocation density were developed by Acharya (2001, 2004), Acharya et al. (2006) and Roy and Acharya (2006); see also a recent development in which a finite deformation formalism was presented (Arora and Acharya, 2019). Formalisms that distinguish dislocations based upon their slip systems but utilize scalar or vector representations of the dislocation fields were developed by other authors (El-Azab, 2006, 2000; Deng and El-Azab, 2010, 2009, 2007; Hochrainer et al., 2014; Po et al., 2019; Sedláček et al., 2007; Xia et al., 2016; Xia and El-Azab, 2015a, 2015b; Zaiser and Hochrainer, 2006). In the latter models, the line direction of dislocations is preserved in the density representation so as to facilitate the incorporation of processes such as cross slip, annihilation, and junction reactions (Monavari et al., 2016; Stricker et al., 2018; Xia et al., 2016). However, most of the latter models, the ones of interest here, lack the kinematics of finite deformation, which is intimately tied to the dislocation patterns in crystals deforming in multiple slip up to strains exceeding few percent. In such strain ranges, crystals develop dislocation microstructures with dislocation dense boundaries. Three characteristic types of such boundaries were observed under monotonic loading: extended planar boundaries aligned with slip planes, microstructures with shorter and more randomly oriented boundaries forming cells, and extended planar boundaries on planes slightly deviating from the slip plane; see Fig. 1. In between the extended planar boundaries cells are also found. All three types of microstructures are observed independent of the deformation mode, e.g., tension (Huang and Hansen, 1997), compression (Le et al., 2012) and rolling (Liu et al., 1998). In all modes, however, the type of microstructure found exhibits a strong dependence on the crystallographic orientation of the load. The microstructures in single crystals of aluminum (Kashihara et al., 1996, Tagami et al., 2000), nickel (Zheng et al., 2016) and copper (Kawasaki and Takeuchi, 1980) exhibit the same type of orientation dependence. It was also observed that grains in polycrystals develop microstructures with the same orientation dependence and microstructural characteristics as single crystals (Hansen and Huang, 1998; Huang and Hansen, 1997) for grain sizes down to about 1 μm (Le et al., 2013). These characteristics have been clearly observed after true strains of about 0.05–0.8 (Huang and Winther, 2007) and strain rates of 10^{-4}–10^{3} (Huang and Winther, 2007; Zheng et al., 2016) at ambient temperatures. At smaller strains, the boundaries are less well-defined but dislocation-rich and dislocation-free domains are formed in multi-slip conditions (Jakobsen, 2006; Steeds, 1966).

The goal of the current effort is to develop a mesoscale plasticity formalism capable of predicting the dislocation microstructures of the types discussed above. An important first step in this regard is to generalize our continuum dislocation dynamics (Xia and El-Azab, 2015a) to account for the kinematics of finite deformation of crystals. In doing so, it is critical to distinguish the dislocation density measures in the reference, microstructural, and deformed crystal configurations and derive their space-time evolution equations accordingly. Our effort builds upon the classical continuum representation of dislocations. As such, we mention here the early contributions reported in Kondo (1952), Nye (1952), Bilby et al. (1958), and Kröner (1959). In these works, dislocations were measured by the incompatibility of the displacement field using the dislocation density tensor, $\boldsymbol{\alpha}$. In the case of small deformation, this tensor, which is known as the Kröner–Nye tensor, is derived from the kinematic definition of Burgers vector, $\mathbf{b}$, as follows:

$$-\mathbf{b} = \oint \mathrm{d}\mathbf{u}^{\mathrm{e}} = \oint \boldsymbol{\beta}^{\mathrm{e}} \mathrm{d}\mathbf{x} = \int \left(\nabla \times \boldsymbol{\beta}^{\mathrm{e}}\right) \cdot \mathrm{d}\mathbf{A} = \int \boldsymbol{\alpha} \cdot \mathrm{d}\mathbf{A}. \tag{1}$$

This yields: $\boldsymbol{\alpha} = -\nabla \times \boldsymbol{\beta}^{e} = \nabla \times \boldsymbol{\beta}^{p}$. In the above, $\boldsymbol{\beta}^{e}$ is the elastic distortion, $d\mathbf{u}^{e}$ is a differential elastic displacement over a differential distance $d\mathbf{x}$ in the crystal, and $d\mathbf{A}$ is a differential area element. Mura (1963), Kosevich (1965) and de Wit (1973b, 1973a) further elaborated the dynamics of dislocations within this framework by introducing a dislocation flux and developing continuity equation for the Kröner–Nye tensor in terms of the dislocation flux (El-Azab and Po, 2018). Relatively recently, an invariant form of the second order dislocation density tensor was developed (Cermelli and Gurtin, 2001) and shown to transform between different crystal configurations in the same way as the stress tensor does. Following that development, gradient plasticity theories making use of the dislocation density tensor were developed (Gurtin, 2010, 2006; Gurtin et al., 2007). In Hochrainer (2013), a formulation of dislocation evolution at finite deformation was introduced in the intermediate space necessitating the use of curvilinear coordinates in a way similar to the works in Bilby et al. (1955) and Kröner (1960) but extended this to the language of differential forms and de Rham currents in the finite deformation setting.

In this paper, we present a new formulation of continuum dislocation dynamics for mesoscale plasticity at finite deformation with vector representation of dislocations. The starting point is the kinematics of incompatible crystal deformation. We identify the incompatibility of deformation, i.e., Burgers vector measure, starting with the additive decomposition of the displacement gradient, which was found to be consistent with the definition based on the multiplicative decomposition of the deformation gradient. In deriving the rate form of crystal incompatibility, which is the continuity equations for the dislocation density tensors, we follow an additive decomposition of the material velocity field as well. It is shown that the additive decomposition of the displacement gradient and the compatibility of the total displacement leads to defining multiple dislocation density tensors that were already used by other authors. It is also shown that, the decomposition of the crystal velocity and its compatibility leads to the definition of the dislocation current and transport equations for the dislocation density tensors. In Appendix A, we demonstrate that the latter derivation is consistent with the transport equations derived in Cermelli and Gurtin (2001) for the microstructure dislocation density tensor. Our formalism is distinctly different from other previous works in that it ends up with the transport equations governing the vector dislocation densities as the basic equations of continuum dislocation dynamics. This required a derivation of a work conjugate driving force for dislocation motion which is similar in form to the Peach-Koehler force. Numerical examples are presented for dislocation fields at finite deformation illustrating the role of the geometric non-linearity and lattice rotation in the context of dislocation mechanics at large deformations. Referential forms of the equations of dislocation statics were used in these examples. However, the continuum dislocation dynamics equations of interest were developed in both referential and spatial forms.

2. Notation and preliminary content

Here we follow the tensor notation and convention used by Gurtin et al. (2010). In the following $\mathbf{T}$ represents a second order tensor field and $\mathbf{v}$ represents a vector field.

$$\mathrm{div}(\mathbf{v}) = \frac{\partial v_i}{\partial x_i} \tag{2}$$

$$\mathrm{curl}(\mathbf{v})_i = \epsilon_{ijk}\frac{\partial v_k}{\partial x_j} \tag{3}$$

$$\mathrm{div}(\mathbf{T})_i = \frac{\partial T_{ij}}{\partial x_j} \tag{4}$$

$$\mathrm{curl}(\mathbf{T})_{ij} = \epsilon_{ipq}\frac{\partial T_{jq}}{\partial x_p} \tag{5}$$

The notation $\mathrm{curl}(\mathbf{T})^{T}$ is used here to denote the transpose of the curl of the second order tensor $\mathbf{T}$.

Some useful identities are shown below ($\mathbf{v}$ and $\mathbf{u}$ are vector fields):

$$\mathrm{curl}(\mathbf{u}\otimes\mathbf{v}) \;= [\mathrm{grad}(\mathbf{u})\mathbf{v}\times]^{T} + \mathrm{curl}(\mathbf{v})\otimes\mathbf{u} \tag{6}$$

$$\mathrm{div}(\mathbf{u}\otimes\mathbf{v}) \;= \mathrm{div}(\mathbf{v})\mathbf{u} + \mathrm{grad}(\mathbf{u})\mathbf{v} \tag{7}$$

$$\mathrm{curl}(\mathbf{u}\times\mathbf{v}) \;= \mathrm{div}(\mathbf{u}\otimes\mathbf{v} - \mathbf{v}\otimes\mathbf{u}) \tag{8}$$

Stokes theorem is expressed in the form:

$$\oint \mathbf{T}d\mathbf{x} = \int \mathrm{curl}(\mathbf{T})^{T}\mathbf{n}da\ , \tag{9}$$

which follows from the well-known Stokes theorem for vector fields,

$$\oint \mathbf{v}\cdot d\mathbf{x} = \int \mathbf{n}\cdot\mathrm{curl}(\mathbf{v})da, \tag{10}$$

with the substitution $\mathbf{v} = \mathbf{Tc}$ for an arbitrary constant vector $\mathbf{c}$ that can be factored out to give (9). In the above $\mathbf{n}$da is an oriented area element with unit normal $\mathbf{n}$ and magnitude da. We refer to the material time derivative operator with the usual superposed dot notation,

$$(\dot{.}) = \frac{\partial}{\partial t}(\,)_{\mathbf{X}}$$

with $\mathbf{X}$ being the position vector in the reference configuration. The definitions (2)–(5) are written with respect to the coordinates $\mathbf{x}$ in the deformed configuration. The spatial differential operators with respect to referential coordinate $\mathbf{X}$ will be denoted by upper case; for example, the divergence of a vector field $\mathbf{v}$ is

$$\mathrm{Div}(\mathbf{v}) = \frac{\partial v_i}{\partial X_i}. \tag{11}$$

We will also use the following tensor identities for the double inner product of two second order tensors $\mathbf{A}$ and $\mathbf{B}$:

$$\mathbf{A} : \mathbf{B} = A_{ij}B_{ij}, \tag{12}$$

from which the identities below follow:

$$\mathbf{A} : \mathbf{B} = \mathbf{A}^{\mathrm{T}} : \mathbf{B}^{\mathrm{T}} \tag{13}$$

$$\mathbf{A} : (\mathbf{BC}) = \left(\mathbf{B}^{\mathrm{T}}\mathbf{A}\right) : \mathbf{C} = \left(\mathbf{AC}^{\mathrm{T}}\right) : \mathbf{B}. \tag{14}$$

3. Incompatible crystal deformation and dislocation density measures

In this section, we introduce several dislocation density measures associated with plastic deformation of crystals, including two-point tensors in addition to that introduced by Cermelli and Gurtin (2001). Unlike these and other authors, we do so by working with the displacement gradient and its elastic and plastic components.

3.1. Decomposition of deformation gradient and displacement gradient

In the finite deformation setting for single crystal plasticity, the Kröner-Lee multiplicative decomposition of the deformation gradient $\mathbf{F}$ (Kröner, 1958; Lee, 1969) is used,

$$\mathbf{F} = \mathrm{Grad}\boldsymbol{\Psi} = \mathbf{F}^{e}\mathbf{F}^{p}, \tag{15}$$

where $\mathbf{F}$ is the referential gradient of the deformation mapping $\mathbf{x} = \boldsymbol{\psi}(\mathbf{X}, t)$, with $\mathbf{X}$ and $\mathbf{x}$ being the position vectors in the reference and deformed configurations of the crystal, respectively, and t is time. The elastic distortion $\mathbf{F}^{e}$ and the plastic distortion $\mathbf{F}^{p}$ are generally incompatible and do not generally represent gradients of a deformation mapping as does $\mathbf{F}$ itself. $\mathbf{F}^{e}$ holds the information of the rotation and stretch of the crystal lattice while $\mathbf{F}^{p}$ holds the information of the deformation due to the creation and motion of defects, mainly dislocations in our case. The decomposition (15) is understood in the sense that $d\mathbf{x} = \mathbf{F}d\mathbf{X}$, $d\mathbf{y} = \mathbf{F}^{p}d\mathbf{X}$, and $d\mathbf{x} = \mathbf{F}^{e}d\mathbf{y}$, with $d\mathbf{X}$ and $d\mathbf{x}$ being differential vector distances in the reference and deformed configurations of the crystal, respectively, and $d\mathbf{y}$ is a corresponding distance in the microstructure (intermediate) space. The latter space is not a continuous configuration of the material that is obtained by the gradient of a mapping from the reference configuration (Gurtin and Reddy, 2016). With this decomposition, the velocity gradient can be written as,

$$\mathbf{L} = \mathrm{grad}\ \mathbf{v} = \mathbf{L}^{e} + \mathbf{F}^{e}\mathbf{L}^{p}\mathbf{F}^{e-1}, \tag{16}$$

where we define the elastic velocity gradient in deformed configuration

$$\mathbf{L}^{e} = \dot{\mathbf{F}}^{e}\mathbf{F}^{e-1} \tag{17}$$

and the plastic velocity gradient in the microstructure space is

$$\mathbf{L}^{p} = \dot{\mathbf{F}}^{p}\mathbf{F}^{p-1}. \tag{18}$$

The kinematic argument that plasticity happens due to slip on specific slip planes manifests itself in the relationship (Rice, 1971),

$$\begin{aligned} \mathbf{L}^{p} &= \sum_{l} \dot{\gamma}^{l}\mathbf{S}^{l} \\ \mathbf{S}^{l} &= \mathbf{s}^{l} \otimes \mathbf{m}^{l} \\ \mathbf{m}^{l} \cdot \mathbf{s}^{l} &= 0,\ \left|\mathbf{s}^{l}\right| = \left|\mathbf{m}^{l}\right| = 1, \end{aligned} \tag{19}$$

with $\mathbf{S}^{l}$ being the Schmid tensor of the l^{th} slip system, $\mathbf{s}^{l}$ is the slip direction and $\mathbf{m}^{l}$ is the slip plane normal in the microstructure space. The term $\mathbf{F}^{e}\mathbf{L}^{p}\mathbf{F}^{e-1}$ in (16) represents the push forward of the plastic velocity gradient in the microstructure space to the deformed configuration. From the multiplicative decomposition the total Lagrangian strain can be decomposed into elastic and plastic parts,

$$\mathbf{E} = \mathbf{F}^{p\mathrm{T}}\mathbf{E}^{e}\mathbf{F}^{p} + \mathbf{E}^{p}, \tag{20}$$

where

$$\mathbf{E}^{\mathrm{p}} = \frac{1}{2}\left(\mathbf{F}^{\mathrm{p}\mathrm{T}}\mathbf{F}^{\mathrm{p}} - \mathbf{I}\right)$$
$$\mathbf{E}^{\mathrm{e}} = \frac{1}{2}\left(\mathbf{F}^{\mathrm{e}\mathrm{T}}\mathbf{F}^{\mathrm{e}} - \mathbf{I}\right). \tag{21}$$

We may also write (20) as $\mathbf{E} = \mathbf{E}_{\mathrm{R}}^{\mathrm{e}} + \mathbf{E}^{\mathrm{p}}$, with $\mathbf{E}_{\mathrm{R}}^{\mathrm{e}} \equiv \mathbf{F}^{\mathrm{p}\mathrm{T}}\mathbf{E}^{\mathrm{e}}\mathbf{F}^{\mathrm{p}}$ being the pullback of the elastic strain in the microstructure space to the reference configuration.

We propose to additively decompose the differential displacement $\mathrm{d}\mathbf{u} = \mathbf{u}(\mathbf{X} + \mathrm{d}\mathbf{X}) - \mathbf{u}(\mathbf{X}) = \mathbf{u}(\mathbf{x} + \mathrm{d}\mathbf{x}) - \mathbf{u}(\mathbf{x})$ along a differential element $\mathrm{d}\mathbf{X}$ into plastic and elastic parts in the form,

$$\mathrm{d}\mathbf{u} = \boldsymbol{\beta}\mathrm{d}\mathbf{X} = \boldsymbol{\beta}^{\mathrm{p}}\mathrm{d}\mathbf{X} + \boldsymbol{\beta}^{\mathrm{e}}\mathrm{d}\mathbf{x} \tag{22}$$

where,

$$\boldsymbol{\beta}^{\mathrm{p}} \equiv \mathbf{F}^{\mathrm{p}} - \mathbf{I} \text{ and } \boldsymbol{\beta}^{\mathrm{e}} \equiv \mathbf{I} - \mathbf{F}^{e-1}. \tag{23}$$

In the above construction, $\boldsymbol{\beta}^{\mathrm{p}}$ and $\boldsymbol{\beta}^{\mathbf{e}}$ coincide with the elastic and plastic distortions of Kröner (1958) in the limit of infinitesimal deformation. We now show that this construction is true by making use of the multiplicative decomposition. Using (22), (23) and (15) we get,

$$\begin{aligned}
\boldsymbol{\beta}^{\mathrm{p}}\mathrm{d}\mathbf{X} + \boldsymbol{\beta}^{\mathrm{e}}\mathrm{d}\mathbf{x} &= (\mathbf{F}^{\mathrm{p}} - \mathbf{I})\mathrm{d}\mathbf{X} + \left(\mathbf{I} - \mathbf{F}^{\mathrm{e}-1}\right)\mathrm{d}\mathbf{x} \\
&= (\mathbf{F}^{\mathrm{p}} - \mathbf{I})\mathrm{d}\mathbf{X} + \left(\mathbf{I} - \mathbf{F}^{\mathrm{e}-1}\right)\mathbf{F}\mathbf{d}\mathbf{X} \\
&= (\mathbf{F}^{\mathrm{p}} - \mathbf{I})\mathrm{d}\mathbf{X} + (\mathbf{F} - \mathbf{F}^{\mathrm{p}})\mathbf{d}\mathbf{X} \\
&= (\mathbf{F} - \mathbf{I})\mathrm{d}\mathbf{X} = \boldsymbol{\beta}\mathrm{d}\mathbf{X} = \mathrm{d}\mathbf{u}.
\end{aligned}$$

We also define the plastic and elastic differential displacements by,

$$d\mathbf{u}^{\mathbf{p}} \equiv \boldsymbol{\beta}^{\mathrm{p}}\mathrm{d}\mathbf{X}$$
$$d\mathbf{u}^{\mathbf{e}} \equiv \boldsymbol{\beta}^{\mathrm{e}}\mathrm{d}\mathbf{x}, \tag{24}$$

so that

$$\mathrm{d}\mathbf{u} = d\mathbf{u}^{\mathrm{p}} + d\mathbf{u}^{\mathrm{e}}. \tag{25}$$

We note that we are distinguishing between the integrable differential $\mathrm{d}\mathbf{u}$ and the non-integrable differentials $d\mathbf{u}^{\mathrm{p}}$ and $d\mathbf{u}^{\mathrm{e}}$ with italicized font. We note here that we can use the Helmholtz decomposition, as was first done in Acharya (2001), in the context of dislocations and plasticity, for second order tensors to write

$$\boldsymbol{\beta}^{\mathrm{p}} = \boldsymbol{\varphi}^{\mathrm{p}} + \boldsymbol{\chi}^{\mathrm{p}} \text{ and } \boldsymbol{\beta}^{\mathrm{e}} = \boldsymbol{\varphi}^{\mathrm{e}} + \boldsymbol{\chi}^{\mathrm{e}}, \tag{26}$$

where,

$$\boldsymbol{\varphi}^{\mathrm{p}} = \mathrm{Grad}\ \mathbf{V}^{\mathrm{p}},\ \ \boldsymbol{\varphi}^{\mathrm{e}} = \mathrm{grad}\ \mathbf{V}^{\mathrm{e}}$$

$$\boldsymbol{\chi}^{\mathrm{p}} = \mathrm{Curl}(\mathbf{A}^{\mathrm{p}})^{\mathrm{T}},\ \boldsymbol{\chi}^{\mathrm{e}} = \mathrm{curl}(\mathbf{A}^{\mathrm{e}})^{\mathrm{T}},$$

with $\mathbf{V}^{\mathrm{p}}$ and $\mathbf{V}^{\mathrm{e}}$ being vector potentials and $\mathbf{A}^{\mathrm{p}}$ and $\mathbf{A}^{\mathrm{e}}$ second order tensor potentials. We note that the Helmholtz decomposition for second order tensors can be traced back to Hauser (1970) where it was introduced in the context of electromagnetism. A consequence of the decomposition (26) for $\boldsymbol{\beta}^{\mathbf{e}}$ and $\boldsymbol{\beta}^{\mathrm{p}}$ is that the elastic and plastic distortions can be written in the form: $\mathbf{F}^{\mathrm{p}} = (\boldsymbol{\varphi}^{\mathrm{p}} - \mathbf{I}) + \boldsymbol{\chi}^{\mathrm{p}}$ and $\mathbf{F}^{e-1} = (\mathbf{I} - \boldsymbol{\varphi}^{\mathrm{e}}) + \boldsymbol{\chi}^{\mathrm{e}}$. In turn,

$$\mathrm{Curl}\left(\boldsymbol{\beta}^{\mathrm{p}}\right) = \mathrm{Curl}(\boldsymbol{\chi}^{\mathrm{p}}) = \mathrm{Curl}(\mathbf{F}^{\mathrm{p}})$$
$$\mathrm{curl}\left(\boldsymbol{\beta}^{\mathrm{e}}\right) = \mathrm{curl}(\boldsymbol{\chi}^{\mathrm{e}}) = -\mathrm{curl}\left(\mathbf{F}^{\mathrm{e}-1}\right). \tag{27}$$

The last equations show that the curl operation isolates the incompatible fields $\boldsymbol{\chi}^{\mathrm{p}}$ and $\boldsymbol{\chi}^{\mathrm{e}}$ which we will relate to the dislocation density in following sections.

3.2. Compatibility conditions and definition of dislocation density tensor

We are now in a position to define the dislocation density tensor by investigating the compatibility of the displacement field and its elastic and plastic contributions. We start with the compatibility condition of the total displacement,

$$\oint \mathrm{d}\mathbf{u} = \oint \boldsymbol{\beta}\mathrm{d}\mathbf{X} = 0, \tag{28}$$

where the integral is carried out along a closed path in the crystal. Using (22) this becomes,

$$\oint \boldsymbol{\beta}\mathrm{d}\mathbf{X} = \oint \boldsymbol{\beta}^{\mathrm{p}}\mathrm{d}\mathbf{X} + \oint \boldsymbol{\beta}^{\mathrm{e}}\mathrm{d}\mathbf{x} = 0 \tag{29}$$

Using Stokes theorem, we reach

$$\int \mathrm{Curl}\left(\boldsymbol{\beta}^{\mathrm{p}}\right)^{\mathrm{T}} \mathrm{d}\mathbf{A}_{\mathrm{R}} + \int \mathrm{curl}\left(\boldsymbol{\beta}^{\mathrm{e}}\right)^{\mathrm{T}} \mathrm{d}\mathbf{a}_{\mathrm{D}} = 0\ . \tag{30}$$

That is,

$$\int \mathrm{Curl}\left(\boldsymbol{\beta}^{\mathrm{p}}\right)^{\mathrm{T}} \mathrm{d}\mathbf{A}_{\mathrm{R}} = -\int \mathrm{curl}\left(\boldsymbol{\beta}^{\mathrm{e}}\right)^{\mathrm{T}} \mathrm{d}\mathbf{a}_{\mathrm{D}}\ . \tag{31}$$

with $\mathrm{d}\mathbf{A}_{\mathrm{R}}$ and $\mathrm{d}\mathbf{a}_{\mathrm{D}}$ being differential area elements in the referential and spatial configurations, respectively. We can then define two-point dislocation density tensors by

$$\begin{aligned} \boldsymbol{\alpha}^{\mathrm{RM}} &\equiv \mathrm{Curl}\left(\boldsymbol{\beta}^{\mathrm{p}}\right) = \mathrm{Curl}\left(\mathbf{F}^{\mathrm{p}}\right) \\ \boldsymbol{\alpha}^{\mathrm{DM}} &\equiv \mathrm{curl}\left(\boldsymbol{\beta}^{\mathrm{e}}\right) = \mathrm{curl}\left(\mathbf{F}^{\mathrm{e}-1}\right), \end{aligned} \tag{32}$$

where $\boldsymbol{\alpha}^{\mathrm{DM}}$ is the dislocation density tensor that Acharya uses in his field dislocation mechanics theory (Acharya, 2001). From this point onward, the superscripts and subscripts R, M and D on vector and tensor quantities refer to their measures in the reference, microstructure and deformed configurations, respectively. Double superscripts on two-point tensors refer to the two configurations they are associated with. We note here that since both $\boldsymbol{\alpha}^{\mathrm{RM}}$ and $\boldsymbol{\alpha}^{\mathrm{DM}}$ are defined to be the curl of tensors they must satisfy:

$$\begin{aligned} &\mathrm{Div}\left(\boldsymbol{\alpha}^{\mathrm{RM\ T}}\right) = 0 \\ &\mathrm{div}\left(\boldsymbol{\alpha}^{\mathrm{DM\ T}}\right) = 0. \end{aligned} \tag{33}$$

These conditions have the usual interpretation that the dislocations have no free ends inside the crystal. It is to be noted here that, according to the definitions of the curl operator we used, and for a second order tensor $\mathbf{T}$, Div $(\mathrm{Curl}(\mathbf{T})^{\mathrm{T}}) = 0$. Hence the transpose in the divergence conditions (33). Some authors define the curl operator so that Div (Curl $\mathbf{T}) = 0$. In addition to the above relations, we can also write the differential Burgers vector in the microstructure configuration as follows:

$$\mathrm{d}\mathbf{b}_{\mathrm{M}} = \boldsymbol{\alpha}^{\mathrm{RM\ T}} \mathrm{d}\mathbf{A}_{\mathrm{R}} = \boldsymbol{\alpha}^{\mathrm{DM\ T}} \mathrm{d}\mathbf{a}_{\mathrm{D}}. \tag{34}$$

Nanson's formula can then be used to arrive at the microstructural dislocation density tensor, $\boldsymbol{\alpha}^{\mathrm{M}}$:

$$\boldsymbol{\alpha}^{\mathrm{M}} \equiv \frac{1}{\mathrm{J}^{\mathrm{p}}} \mathbf{F}^{\mathrm{p}} \mathrm{Curl}\left(\boldsymbol{\beta}^{\mathrm{p}}\right) = \frac{1}{\mathrm{J}^{\mathrm{p}}} \mathbf{F}^{\mathrm{p}} \mathrm{Curl}\left(\mathbf{F}^{\mathrm{p}}\right) = \mathrm{J}^{\mathrm{e}} \mathbf{F}^{\mathbf{e}-1} \mathrm{curl}\left(\boldsymbol{\beta}^{\mathbf{e}}\right) = \mathrm{J}^{\mathrm{e}} \mathbf{F}^{e-1} \mathrm{curl}\left(\mathbf{F}^{e-1}\right), \tag{35}$$

where the last terms come from (27). We note that these are the same definitions that Cermelli and Gurtin (2001) made. The tensor $\boldsymbol{\alpha}^{\mathrm{M}}$ lives in the microstructure space and gives a local measure of Burgers vector $\mathbf{b}_{\mathrm{M}}$ in that space through the relation

$$\mathrm{d}\mathbf{b}_{\mathrm{M}} = \boldsymbol{\alpha}^{\mathrm{M\ T}} \mathrm{d}\mathbf{A}_{\mathrm{M}}. \tag{36}$$

It is now possible to derive relations for the referential dislocation density tensor and the deformed dislocation density tensor using the same ideas in Cermelli and Gurtin (2001). The microstructure Burgers vector $\mathrm{d}\mathbf{b}_{\mathrm{M}}$ can be transformed into either its deformed $\mathrm{d}\mathbf{b}_{\mathrm{D}}$ or referential $\mathrm{d}\mathbf{b}_{\mathrm{M}}$ counterpart via

$$\begin{aligned} \mathrm{d}\mathbf{b}_{\mathrm{R}} &= \mathbf{F}^{\mathrm{p}-1} \mathrm{d}\mathbf{b}_{\mathrm{M}} \\ \mathrm{d}\mathbf{b}_{\mathrm{D}} &= \mathbf{F}^{\mathrm{e}} \mathrm{d}\mathbf{b}_{\mathrm{M}}. \end{aligned} \tag{37}$$

Furthermore, using Nanson's formula, we can transform the microstructure area element into referential and deformed area elements which allows us to write

$$\begin{aligned} \mathrm{d}\mathbf{b}_{\mathrm{M}} &= \boldsymbol{\alpha}^{\mathrm{MT}} \mathrm{J}^{\mathrm{p}} \mathbf{F}^{\mathrm{p}-\mathrm{T}} \mathrm{d}\mathbf{A}_{\mathrm{R}} \\ \mathrm{d}\mathbf{b}_{\mathrm{M}} &= \boldsymbol{\alpha}^{\mathrm{MT}} \frac{1}{\mathrm{J}^{\mathrm{e}}} \mathbf{F}^{\mathrm{eT}} \mathrm{d}\mathbf{A}_{\mathrm{D}}. \end{aligned} \tag{38}$$

Combining (37) and (38) gives us the definition of the dislocation density tensor in the reference and deformed configuration,

$$\begin{aligned} \mathrm{d}\mathbf{b}_{\mathrm{R}} &= \mathbf{F}^{\mathrm{p}-1} \mathrm{Curl}\left(\mathbf{F}^{\mathrm{p}}\right)^{\mathrm{T}} \mathrm{d}\mathbf{A}_{\mathrm{R}} \equiv \boldsymbol{\alpha}^{\mathrm{RT}} \mathrm{d}\mathbf{A}_{\mathrm{R}} \\ \mathrm{d}\mathbf{b}_{\mathrm{D}} &= \mathbf{F}^{\mathrm{e}} \mathrm{curl}\left(\mathbf{F}^{\mathrm{e}-1}\right)^{\mathrm{T}} \mathrm{d}\mathbf{A}_{\mathrm{D}} \equiv \boldsymbol{\alpha}^{\mathrm{DT}} \mathrm{d}\mathbf{A}_{\mathrm{D}}. \end{aligned} \tag{39}$$

From these transformations we get the following relationships:

$$\begin{aligned} \boldsymbol{\alpha}^{\mathrm{R}} &= \mathrm{J}^{\mathrm{p}} \mathbf{F}^{\mathrm{p}-1} \boldsymbol{\alpha}^{\mathrm{M}} \mathbf{F}^{\mathrm{p}-\mathrm{T}} \quad \boldsymbol{\alpha}^{\mathrm{M}} = \mathrm{J}^{\mathrm{p}-1} \mathbf{F}^{\mathrm{p}} \boldsymbol{\alpha}^{\mathrm{R}} \mathbf{F}^{\mathrm{pT}} \\ \boldsymbol{\alpha}^{\mathrm{D}} &= \mathrm{J}^{\mathrm{e}-1} \mathbf{F}^{\mathrm{e}} \boldsymbol{\alpha}^{\mathrm{M}} \mathbf{F}^{\mathrm{eT}} \quad \boldsymbol{\alpha}^{\mathrm{M}} = \mathrm{J}^{\mathrm{e}} \mathbf{F}^{\mathrm{e}-1} \boldsymbol{\alpha}^{\mathrm{D}} \mathbf{F}^{\mathrm{e}-\mathrm{T}} \\ \boldsymbol{\alpha}^{\mathrm{R}} &= \mathrm{J}\, \mathbf{F}^{-1} \boldsymbol{\alpha}^{\mathrm{D}} \mathbf{F}^{-\mathrm{T}} \quad \boldsymbol{\alpha}^{\mathrm{D}} = \mathrm{J}^{-1} \mathbf{F}\, \boldsymbol{\alpha}^{\mathrm{R}} \mathbf{F}^{\mathrm{T}} \end{aligned}$$

$$\begin{aligned}\boldsymbol{\alpha}^{\mathrm{RM}} &= \mathrm{J}^{\mathrm{p}}\mathbf{F}^{\mathrm{p}-1}\boldsymbol{\alpha}^{\mathrm{M}} \quad \boldsymbol{\alpha}^{\mathrm{M}} = \mathrm{J}^{\mathrm{p}\ -1}\mathbf{F}^{\mathrm{p}}\boldsymbol{\alpha}^{\mathrm{RM}} \\ \boldsymbol{\alpha}^{\mathrm{DM}} &= \mathrm{J}^{\mathrm{e}-1}\mathbf{F}^{\mathrm{e}}\boldsymbol{\alpha}^{\mathrm{M}} \quad \boldsymbol{\alpha}^{\mathrm{M}} = \mathrm{J}^{\mathrm{e}}\mathbf{F}^{\mathrm{e}-1}\boldsymbol{\alpha}^{\mathrm{DM}}.\end{aligned} \tag{40}$$

The connections between $\boldsymbol{\alpha}^{\mathrm{M}}, \boldsymbol{\alpha}^{\mathrm{D}}$ and $\boldsymbol{\alpha}^{\mathrm{R}}$ were given by Cermelli and Gurtin (2001). These dislocation density tensors can be written as compositions of vector dislocation densities in the respective crystal configurations and the corresponding crystallographic Burgers vectors. In order to do so, we assume that the dislocation density on each crystallographic slip system consists of line bundles having single-valued line direction at each point in space. For simplicity, let us assume that we have a single slip system with crystallographic Burgers vector $\mathbf{b}_{\mathrm{R}}$, in the reference configuration, with its images in the microstructure and deformed configurations being $\mathbf{b}_{\mathrm{M}}$ and $\mathbf{b}_{\mathrm{D}}$, respectively. In this case, the dislocation density tensors mentioned above have the form

$$\begin{aligned}\boldsymbol{\alpha}^{\mathrm{R}} &= \boldsymbol{\rho}_{\mathrm{R}} \otimes \mathbf{b}_{\mathrm{R}} = \rho_{\mathrm{R}}\mathbf{l}_{\mathrm{R}} \otimes \mathbf{b}_{\mathrm{R}} \\ \boldsymbol{\alpha}^{\mathrm{M}} &= \boldsymbol{\rho}_{\mathrm{M}} \otimes \mathbf{b}_{\mathrm{M}} = \rho_{\mathrm{M}}\ \mathbf{l}_{\mathrm{M}} \otimes \mathbf{b}_{\mathrm{M}} \\ \boldsymbol{\alpha}^{\mathrm{D}} &= \boldsymbol{\rho}_{\mathrm{D}} \otimes \mathbf{b}_{\mathrm{D}} = \rho_{\mathrm{D}}\ \mathbf{l}_{\mathrm{D}} \otimes \mathbf{b}_{\mathrm{D}} \\ \boldsymbol{\alpha}^{\mathrm{RM}} &= \boldsymbol{\rho}_{\mathrm{R}} \otimes \mathbf{b}_{\mathrm{M}} = \rho_{\mathrm{R}}\mathbf{l}_{\mathrm{R}} \otimes \mathbf{b}_{\mathrm{M}} \\ \boldsymbol{\alpha}^{\mathrm{DM}} &= \boldsymbol{\rho}_{\mathrm{D}} \otimes \mathbf{b}_{\mathrm{M}} = \rho_{\mathrm{D}}\ \mathbf{l}_{\mathrm{D}} \otimes \mathbf{b}_{\mathrm{M}},\end{aligned} \tag{41}$$

where $\boldsymbol{\rho}_{\mathrm{R}}$, $\boldsymbol{\rho}_{\mathrm{M}}$, and $\boldsymbol{\rho}_{\mathrm{D}}$ are the vector dislocation densities in the reference, microstructure and deformed configurations with their magnitudes ρ_{R}, ρ_{M} , and ρ_{D} and unit tangents $\mathbf{l}_{\mathrm{R}}$, $\mathbf{l}_{\mathrm{M}}$, and $\mathbf{l}_{\mathrm{D}}$, respectively. When multiple slip systems are considered, expressions (41) are constructed by summing the contributions from all systems; see Section 5.

We also have the transformation relations:

$$\begin{aligned}&\mathbf{l}_{\mathrm{R}} = \mathbf{F}^{\mathrm{p}-1}\mathbf{l}_{\mathrm{M}} && \mathbf{s}_{\mathrm{R}} = \mathbf{F}^{\mathrm{p}-1}\mathbf{s}_{\mathrm{M}} && \mathbf{m}_{\mathrm{R}} = \mathbf{F}^{\mathrm{p}\mathrm{T}}\mathbf{m}_{\mathrm{M}} \\ &\mathbf{l}_{\mathrm{D}} = \mathbf{F}^{\mathrm{e}}\mathbf{l}_{\mathrm{M}} && \mathbf{s}_{\mathrm{D}} = \mathbf{F}^{\mathrm{e}}\mathbf{s}_{\mathrm{M}} && \mathbf{m}_{\mathrm{D}} = \mathbf{F}^{\mathrm{e}-\mathrm{T}}\mathbf{m}_{\mathrm{M}} \\ &\mathbf{l}_{\mathrm{D}} = \mathbf{F}\mathbf{l}_{\mathrm{R}} && \mathbf{s}_{\mathrm{D}} = \mathbf{F}\mathbf{s}_{\mathrm{R}}, && \mathbf{m}_{\mathrm{D}} = \mathbf{F}^{-\mathrm{T}}\mathbf{m}_{\mathrm{R}} \\ &\mathbf{b}_{\mathrm{R}} = \mathrm{b}\mathbf{s}_{\mathrm{R}} && \mathbf{b}_{\mathrm{M}} = \mathrm{b}\mathbf{s}_{\mathrm{M}} && \mathbf{b}_{\mathrm{D}} = \mathrm{b}\mathbf{s}_{\mathrm{D}} \\ &\boldsymbol{\rho}_{\mathrm{R}} = \mathrm{J}^{\mathrm{p}}\mathbf{F}^{\mathbf{p}-1}\boldsymbol{\rho}_{\mathbf{M}} && \boldsymbol{\rho}_{\mathbf{D}} = \mathrm{J}^{\mathrm{e}-1}\mathbf{F}^{\mathbf{e}}\boldsymbol{\rho}_{\mathbf{M}} && \boldsymbol{\rho}_{\mathbf{R}} = \mathrm{J}\mathbf{F}^{-1}\boldsymbol{\rho}_{\mathbf{D}}.\end{aligned} \tag{42}$$

As seen in the following sections, these relations are useful in deriving the transport relations for the dislocation density. Again, the subscripts R, M and D refer to the reference, microstructure and deformed configurations, respectively.

4. Dislocation currents and continuity equations for the dislocation density tensors

The crystal displacement field is compatible and so is the corresponding velocity field. This means that

$$\oint \mathrm{d}\mathbf{v} = \oint \dot{\boldsymbol{\beta}}\mathrm{d}\mathbf{X} = \overline{\oint \boldsymbol{\beta}\mathrm{d}\mathbf{X}}^{\,\cdot} = 0. \tag{43}$$

For d$\mathbf{v}$, we use the differential definition of the velocity, (Reddy, 2013)

$$\mathrm{d}\mathbf{v} = \overline{\mathrm{d}\mathbf{x}}^{\,\cdot} = \overline{\mathbf{F}\mathrm{d}\mathbf{X}}^{\,\cdot} = \overline{\boldsymbol{\beta}\mathrm{d}\mathbf{X}}^{\,\cdot}. \tag{44}$$

We now use our additive decomposition of the displacement gradient to show how the incompatible part of the displacement gradient should evolve. To this end, we write

$$\begin{aligned}\overline{\boldsymbol{\beta}\mathrm{d}\mathbf{X}}^{\,\cdot} &= \overline{\boldsymbol{\beta}^{\mathrm{p}}\mathrm{d}\mathbf{X} + \boldsymbol{\beta}^{\mathbf{e}}\mathrm{d}\mathbf{x}}^{\,\cdot} \\ &= \overline{\boldsymbol{\beta}^{\mathrm{p}}\mathrm{d}\mathbf{X}}^{\,\cdot} + \overline{\boldsymbol{\beta}^{\mathrm{e}}\mathbf{F}\mathrm{d}\mathbf{X}}^{\,\cdot} \\ &= \dot{\boldsymbol{\beta}}^{\mathrm{p}}\mathrm{d}\mathbf{X} + \left(\dot{\boldsymbol{\beta}}^{\mathrm{e}}\ \mathrm{d}\mathbf{x} + \boldsymbol{\beta}^{\mathrm{e}}\mathbf{L}\mathbf{F}\mathrm{d}\mathbf{X}\right) \\ &= \dot{\boldsymbol{\beta}}^{\mathrm{p}}\mathrm{d}\mathbf{X} + \left(\dot{\boldsymbol{\beta}}^{\mathrm{e}} + \boldsymbol{\beta}^{\mathrm{e}}\mathbf{L}\right)\mathrm{d}\mathbf{x}.\end{aligned} \tag{45}$$

We start by simplifying the quantity $(\dot{\boldsymbol{\beta}}^{\mathrm{e}} + \boldsymbol{\beta}^{\mathrm{e}}\mathbf{L})\mathrm{d}\mathbf{x}$ in the above expression. We find the first term to be

$$\dot{\boldsymbol{\beta}}^{\mathrm{e}} = -\dot{\mathbf{F}}^{\mathrm{e}-1} = \mathbf{F}^{\mathrm{e}-1}\mathbf{L}^{\mathrm{e}}, \tag{46}$$

and the second term

$$\begin{aligned}\boldsymbol{\beta}^{\mathrm{e}}\mathbf{L} &= \mathbf{L} - \mathbf{F}^{\mathrm{e}-1}\mathbf{L} \\ &= \mathbf{L} - \mathbf{F}^{\mathrm{e}-1}\mathbf{L}^{\mathrm{e}} - \mathbf{F}^{\mathrm{e}-1}\mathbf{F}^{\mathrm{e}}\mathbf{L}^{\mathrm{p}}\mathbf{F}^{\mathrm{e}-1} = \mathbf{L} - \mathbf{F}^{\mathrm{e}-1}\mathbf{L}^{\mathrm{e}} - \mathbf{L}^{\mathrm{p}}\mathbf{F}^{\mathrm{e}-1}.\end{aligned} \tag{47}$$

Summing (46) and (47) then gives,

$$\begin{aligned}\dot{\boldsymbol{\beta}}^{\mathrm{e}}+\boldsymbol{\beta}^{\mathrm{e}}\mathbf{L}&=\mathbf{F}^{\mathrm{e}-1}\mathbf{L}^{\mathrm{e}}+\mathbf{L}-\mathbf{F}^{\mathrm{e}-1}\mathbf{L}^{\mathrm{e}}-\mathbf{L}^{\mathrm{p}}\mathbf{F}^{\mathrm{e}-1}\\&=\mathbf{L}-\mathbf{L}^{\mathrm{p}}\mathbf{F}^{\mathrm{e}-1}=\mathbf{L}-\mathbf{L}^{\mathrm{p}}\mathbf{F}^{\mathrm{p}}\mathbf{F}^{\mathbf{p}-1}\mathbf{F}^{\mathrm{e}-1}\\&=\mathbf{L}-\dot{\boldsymbol{\beta}}^{\mathrm{p}}\mathbf{F}^{\mathrm{p}-1}\mathbf{F}^{\mathrm{e}-1}=\mathbf{L}-\dot{\boldsymbol{\beta}}^{\mathrm{p}}\mathbf{F}^{-1}.\end{aligned}\tag{48}$$

We now define the plastic and elastic velocity contributions as,

$$\begin{aligned}d\mathbf{v}^{\mathrm{p}}&\equiv\dot{\boldsymbol{\beta}}^{\mathrm{p}}\mathrm{d}\mathbf{X}\\d\mathbf{v}^{\mathrm{e}}&\equiv\left(\mathbf{L}-\dot{\boldsymbol{\beta}}^{\mathrm{p}}\mathbf{F}^{-1}\right)\mathrm{d}\mathbf{x},\end{aligned}\tag{49}$$

which yield,

$$\mathrm{d}\mathbf{v}=d\mathbf{v}^{\mathrm{e}}+d\mathbf{v}^{\mathrm{p}}.\tag{50}$$

where, again, we used italicized font to refer to the fact that $d\mathbf{v}^{\mathrm{e}}$ and $d\mathbf{v}^{\mathrm{p}}$ are not individually rates of compatible displacement fields. The decomposition (50) is used below to derive the dislocation current.

4.1. The dislocation current

In Kossecka and de Wit (1977) the dislocation current is regarded as a measure of the deviation of the rate of plastic distortion from compatibility. Here, we develop the same idea in the finite deformation setting by obtaining a measure of the incompatibility of the plastic contribution to the crystal velocity. Since the crystal velocity is compatible, it is possible to write

$$\oint\mathrm{d}\mathbf{v}=\oint d\mathbf{v}^{\mathrm{p}}+\oint d\mathbf{v}^{\mathrm{e}}=0.\tag{51}$$

That is,

$$\oint d\mathbf{v}^{\mathrm{p}}=-\oint d\mathbf{v}^{\mathrm{e}}.\tag{52}$$

Plugging in the definition of $d\mathbf{v}^{\mathrm{p}}$ and $d\mathbf{v}^{\mathrm{e}}$ from (49) gives,

$$\oint\dot{\boldsymbol{\beta}}^{\mathrm{p}}\mathrm{d}\mathbf{X}=-\oint\left(\mathbf{L}-\dot{\boldsymbol{\beta}}^{\mathrm{p}}\mathbf{F}^{-1}\right)\mathrm{d}\mathbf{x}.\tag{53}$$

Applying Stokes Theorem on both sides we reach,

$$\int\mathrm{Curl}\left(\dot{\boldsymbol{\beta}}^{\mathrm{p}}\right)^{\mathrm{T}}\mathrm{d}\mathbf{A}_{\mathrm{R}}=-\int\mathrm{curl}\left(-\dot{\boldsymbol{\beta}}^{\mathrm{p}}\mathbf{F}^{-1}\right)^{\mathrm{T}}\mathrm{d}\mathbf{a}_{\mathrm{D}},\tag{54}$$

where $\mathrm{d}\mathbf{a}_{\mathrm{D}}=\mathbf{n}_{\mathrm{D}}\mathrm{d}a_{\mathrm{D}}$ and $\mathrm{d}\mathbf{A}_{\mathrm{R}}=\mathbf{N}_{\mathrm{R}}\mathrm{d}A_{\mathbf{R}}$, with $\mathbf{n}_{\mathrm{D}}$ and $\mathbf{N}_{\mathrm{R}}$ being the unit normal in the deformed and reference configurations, respectively, and the contribution due to $\mathbf{L}$ is null since it is compatible. We further note that the term on the left-hand (right-hand) side of (54) is a measure of the incompatibility of the plastic (elastic) part of the velocity. We interpret the left-hand side of (56) as the material time rate of change of the net microstructure Burgers vector $\mathbf{b}_{\mathrm{M}}(A_{\mathrm{R}})$ of dislocations piercing an area A_{R}. Likewise, the right-hand side of (53) defines the same for dislocations piercing an area a_{D} in the deformed configuration, which is the image of A_{R}. This is written as

$$\begin{aligned}\dot{\mathbf{b}}_{\mathrm{M}}(A_{\mathrm{R}})&=\int\mathrm{Curl}\left(\dot{\boldsymbol{\beta}}^{\mathrm{p}}\right)^{\mathrm{T}}\mathrm{d}\mathbf{A}_{\mathrm{R}}\\\dot{\mathbf{b}}_{\mathrm{M}}(a_{\mathrm{D}})&=\int\mathrm{curl}\left(\dot{\boldsymbol{\beta}}^{\mathrm{p}}\mathbf{F}^{-1}\right)^{\mathrm{T}}\mathrm{d}\mathbf{a}_{\mathrm{D}}.\end{aligned}\tag{55}$$

In the above, $\dot{\mathbf{b}}_{\mathrm{M}}(A_{\mathrm{R}})=\dot{\mathbf{b}}_{\mathrm{M}}(a_{\mathrm{D}})$.

Now consider the first of (55). From the decomposition of $\boldsymbol{\beta}^{\mathrm{p}}$ into compatible and incompatible parts (27), we may write,

$$\int\mathrm{Curl}\left(\dot{\boldsymbol{\beta}}^{\mathrm{p}}\right)^{\mathrm{T}}\mathrm{d}\mathbf{A}_{\mathrm{R}}=\int\mathrm{Curl}\left(\dot{\boldsymbol{\chi}}^{\mathrm{p}}\right)^{\mathrm{T}}\mathrm{d}\mathbf{A}_{\mathrm{R}}.\tag{56}$$

We interpret the term $\mathrm{Curl}(\dot{\boldsymbol{\chi}}^{\mathrm{p}})^{\mathrm{T}}$ as coming from motion of dislocations. Using Stokes theorem, we can write this as a flux term ϕ of dislocations piercing a Burgers circuit. That is,

$$\int\mathrm{Curl}\left(\dot{\boldsymbol{\chi}}^{\mathrm{p}}\right)^{\mathrm{T}}\mathrm{d}\mathbf{A}_{\mathbf{R}}=\oint\dot{\boldsymbol{\beta}}^{\mathrm{p}}\mathrm{d}\mathbf{X}\equiv\oint\phi\mathrm{d}\mathbf{X}=\int\mathrm{Curl}(\phi)^{\mathrm{T}}\mathrm{d}\mathbf{A}_{\mathrm{R}}.\tag{57}$$

The term ϕ has been called the dislocation current in Kossecka and de Wit (1977) and so we stick with this term noting that our case is concerned with finite deformations. For the line bundle representation of dislocations on various slip systems, and at a point the crystal, we may express the current ϕ at a point the crystal in terms of the vector densities of these bundles, their velocities, and Burgers vectors in the form (Mura, 1963):

$$\phi = \sum_l \mathbf{b}_{\mathrm{M}}^{(l)} \otimes \left(\mathbf{v}_{\mathrm{R}}^{(l)} \times \boldsymbol{\rho}_{\mathrm{R}}^{(l)}\right), \tag{58}$$

with

$$\mathrm{b}_{\mathrm{M}}^{(l)} \mathbf{v}_{\mathrm{R}}^{(l)} \times \boldsymbol{\rho}_{\mathrm{R}}^{(l)} = \dot{\gamma}^{(l)} \mathbf{m}_{\mathrm{R}}^{(l)}, \tag{59}$$

where $\dot{\gamma}^{(l)}$ is the slip rate on slip system l, with Burgers vector $\mathbf{b}_{\mathrm{M}}^{(l)}$, velocity $\mathbf{v}_{\mathrm{R}}^{(l)}$, and dislocation density $\boldsymbol{\rho}_{\mathrm{R}}^{(l)}$, respectively. We will now consider the current term that comes from the deformed configuration on the right-hand side of (54), $\mathrm{curl}(\phi\mathbf{F}^{-1})^{\mathrm{T}}$, which we wish to write in terms of the dislocation density and velocity vectors in the deformed configuration. To this end we expand the term $\phi\mathbf{F}^{-1}$ to get,

$$\phi\mathbf{F}^{-1} = \left[\sum_l \mathbf{b}_{\mathrm{M}}^{(l)} \otimes \left(\mathbf{v}_{\mathrm{R}}^{(l)} \times \boldsymbol{\rho}_{\mathrm{R}}^{(l)}\right)\right]\mathbf{F}^{-1} = \sum_l \mathbf{b}_{\mathrm{M}}^{(l)} \otimes \left(\left(\mathbf{v}_{\mathrm{R}}^{(l)} \times \boldsymbol{\rho}_{\mathrm{R}}^{(l)}\right)\mathbf{F}^{-1}\right). \tag{60}$$

In index notation, the terms on the right of the outer product read: $[(\mathbf{v}_{\mathrm{R}}^{(l)} \times \boldsymbol{\rho}_{\mathrm{R}}^{(l)})\mathbf{F}^{-1}]_{\mathrm{o}} = \epsilon_{\mathrm{IJK}} \mathrm{v}_{\mathrm{R\ I}}^{(l)} \rho_{\mathrm{R\ J}}^{(l)} \mathrm{F}_{\mathrm{Ko}}^{-1}$. Using the transformation properties of $\rho_{\mathrm{R\ j}}^{(l)}$ in (42) and $\mathrm{v}_{\mathrm{R\ i}}^{(l)}$ from ($\mathbf{F}\mathbf{v}_{\mathrm{R}}^{(l)} = \mathbf{v}_{\mathrm{D}}^{(l)}$), we can rewrite the flux term in terms of the density and dislocation velocity in the deformed configuration,

$$\epsilon_{\mathrm{IJK}} \mathrm{v}_{\mathrm{R\ I}}^{(l)} \rho_{\mathrm{R\ J}}^{(l)} \mathrm{F}_{\mathrm{Ko}}^{-1} = \mathrm{v}_{\mathrm{D\ i}}^{(l)} \rho_{\mathrm{D\ j}}^{(l)} \mathrm{J} \epsilon_{\mathrm{IJK}} \mathrm{F}_{\mathrm{Ii}}^{-1} \mathrm{F}_{\mathrm{Jj}}^{-1} \mathrm{F}_{\mathrm{Ko}}^{-1}. \tag{61}$$

The transformation property of the permutation symbol from spatial to material coordinates, $\epsilon_{\mathrm{IJK}} = \mathrm{J}^{-1} \epsilon_{\mathrm{lmn}} \mathrm{F}_{\mathrm{lI}} \mathrm{F}_{\mathrm{mJ}} \mathrm{F}_{\mathrm{nK}}$, can now be used in (61) to obtain

$$\left[\left(\mathbf{v}_{\mathrm{R}}^{(l)} \times \boldsymbol{\rho}_{\mathrm{R}}^{(l)}\right)\mathbf{F}^{-1}\right]_{\mathrm{o}} = \mathrm{v}_{\mathrm{D\ i}}^{(l)} \rho_{\mathrm{D\ j}}^{(l)} \mathrm{J}\mathrm{J}^{-1} \epsilon_{\mathrm{lmn}} \mathrm{F}_{\mathrm{lI}} \mathrm{F}_{\mathrm{mJ}} \mathrm{F}_{\mathrm{nK}} \mathrm{F}_{\mathrm{Ii}}^{-1} \mathrm{F}_{\mathrm{Jj}}^{-1} \mathrm{F}_{\mathrm{Ko}}^{-1} = \mathrm{v}_{\mathrm{D\ i}}^{(l)} \rho_{\mathrm{D\ j}}^{(l)} \epsilon_{\mathrm{ijo}}. \tag{62}$$

Using this result, we can write the dislocation current term in the deformed configuration as,

$$\mathrm{curl}\left(\phi\mathbf{F}^{-1}\right)^{\mathrm{T}} = \mathrm{curl}\left(\sum_l \mathbf{b}_{\mathrm{M}}^{(l)} \otimes \left(\mathbf{v}_{\mathrm{D}}^{(l)} \times \boldsymbol{\rho}_{\mathrm{D}}^{(l)}\right)\right)^{\mathrm{T}}, \tag{63}$$

with the corresponding vector form of Orowan's equation in the deformed configuration,

$$\mathrm{b}_{\mathrm{M}}^{(l)} \mathbf{v}_{\mathrm{D}}^{(l)} \times \boldsymbol{\rho}_{\mathrm{D}}^{(l)} = \dot{\gamma}^{(l)} \mathbf{m}_{\mathrm{D}}^{(l)}, \tag{64}$$

which is consistent with the transformation rule for $\mathbf{m}_{\mathrm{D}}^{(l)}$ and $\mathbf{m}_{\mathrm{R}}^{(l)}$. The dislocation current is used to describe the time rate of change of Burgers vector content within the body and will be used to get a closed form of transport relations in the following section.

4.2. The rate form of compatibility and the transport equations for the two-point dislocation density tensors

From (34) we can write the time rate of change of the Burgers vector measure coming from both the reference and deformed configuration as,

$$\dot{\overline{\mathrm{d}\mathbf{b}_{\mathrm{M}}}} = \dot{\overline{\boldsymbol{\alpha}^{\mathrm{RM\ T}} \mathrm{d}\mathbf{A}_{\mathrm{R}}}} = \dot{\boldsymbol{\alpha}}^{\mathrm{RM\ T}} \mathrm{d}\mathbf{A}_{\mathrm{R}}, \tag{65}$$

and from the deformed configuration we have,

$$\dot{\overline{\mathrm{d}\mathbf{b}_{\mathbf{M}}}} = \dot{\overline{\boldsymbol{\alpha}^{\mathrm{DM\ T}} \mathrm{d}\mathbf{a}_{\mathrm{D}}}} = \dot{\boldsymbol{\alpha}}^{\mathrm{DM\ T}} \mathrm{d}\mathbf{a}_{\mathrm{D}} \ + \boldsymbol{\alpha}^{\mathrm{DM\ T}} \dot{\overline{\mathrm{d}\mathbf{a}_{\mathrm{D}}}}, \tag{66}$$

where $\dot{\overline{\mathrm{d}\mathbf{a}_{\mathrm{D}}}} = (\mathrm{tr}(\mathbf{L})\mathbf{I} - \mathbf{L}^{\mathrm{T}})\mathrm{d}\mathbf{a}_{\mathrm{D}}$, which we get from the material time derivative of Nanson's formula,

$$\begin{aligned}
\dot{\overline{\mathbf{n}_{\mathrm{D}} \mathrm{d}a_{\mathrm{D}}}} &= \dot{\overline{\mathrm{J}\mathbf{F}^{-\mathrm{T}} \mathbf{N} \mathrm{d}A_{\mathrm{R}}}} \\
&= \dot{\mathrm{J}}\mathbf{F}^{-\mathrm{T}} \mathbf{N} \mathrm{d}A_{\mathrm{R}} + \mathrm{J}\,\dot{\overline{\mathbf{F}^{-\mathrm{T}}}}\, \mathbf{N} \mathrm{d}A_{\mathrm{R}} \\
&= \mathrm{tr}(\mathbf{L})\mathbf{F}^{-\mathrm{T}} \mathbf{N} \mathrm{d}A_{\mathrm{R}} + \left(-\mathbf{L}^{\mathrm{T}} \mathbf{F}^{-\mathrm{T}} \mathbf{N} \mathrm{d}A_{\mathrm{R}}\right) \\
&= \left[\mathrm{tr}(\mathbf{L})\mathbf{I} - \mathbf{L}^{\mathrm{T}}\right]\mathbf{F}^{-\mathrm{T}} \mathbf{N} \mathrm{d}A_{\mathrm{R}} \\
&= \left[\mathrm{tr}(\mathbf{L})\mathbf{I} - \mathbf{L}^{\mathrm{T}}\right]\mathbf{n} \mathrm{d}a_{\mathrm{D}}.
\end{aligned}$$

Plugging this back into (66) yields,

$$\dot{\overline{\mathrm{d}\mathbf{b}_{\mathrm{M}}}} = \left[\dot{\boldsymbol{\alpha}}^{\mathrm{DM\ T}} + \boldsymbol{\alpha}^{\mathrm{DM\ T}}\left(\mathrm{tr}(\mathbf{L})\mathbf{I} - \mathbf{L}^{\mathrm{T}}\right)\right]\mathrm{d}\mathbf{a}_{\mathrm{D}}. \tag{67}$$

For the total velocity to remain compatible, we must maintain the relations,

$$\overline{\mathrm{d}\mathbf{b}_{\mathrm{M}}}^{\cdot} = \mathrm{Curl}(\phi)^{\mathrm{T}}\mathrm{d}\mathbf{A}_{\mathrm{R}}, \tag{68}$$

which says that the net change of the burgers vector content is due to the motion of dislocations, or that the time rate of change of the incompatible part of $\boldsymbol{\beta}^{\mathrm{p}}$ is equal to the incompatible part of the plastic velocity. Using the first equation in (34) and (68) we can write,

$$\int \dot{\boldsymbol{\alpha}}^{\mathrm{RM}\ \mathrm{T}}\mathrm{d}\mathbf{A}_{\mathrm{R}} = \int \mathrm{Curl}(\phi)^{\mathrm{T}}\mathrm{d}\mathbf{A}_{\mathrm{R}}. \tag{69}$$

Locally we then get,

$$\dot{\boldsymbol{\alpha}}^{\mathrm{RM}} = \mathrm{Curl}(\phi)\ . \tag{70}$$

Noting that the rate of plastic distortion, $\dot{\boldsymbol{\beta}}^{\mathrm{p}}$, is equal to the dislocation current, ϕ, the last equation can be regarded as the rate form of the incompatibility of the plastic distortion, expressed in terms of the two-point tensor $\boldsymbol{\alpha}^{\mathrm{RM}}$. We can also derive a similar equation for $\boldsymbol{\alpha}^{\mathrm{DM}}$ from equating (55) and (65) and also noting $\dot{\boldsymbol{\beta}}^{\mathrm{p}} = \phi$. This gives,

$$\int \dot{\boldsymbol{\alpha}}^{\mathrm{DM}\ \mathrm{T}} + \boldsymbol{\alpha}^{\mathrm{DM}\ \mathrm{T}}\left(\mathrm{tr}(\mathbf{L})\mathbf{I} - \mathbf{L}^{\mathrm{T}}\right)\mathrm{d}\mathbf{a}_{\mathrm{D}}\ = \int \mathrm{curl}\left(\phi\mathbf{F}^{-1}\right)^{\mathrm{T}}\mathrm{d}\mathbf{a}_{\mathrm{D}} \tag{71}$$

and locally we have, by taking the transpose,

$$\dot{\boldsymbol{\alpha}}^{\mathrm{DM}} + (\mathrm{tr}(\mathbf{L})\mathbf{I} - \mathbf{L})\boldsymbol{\alpha}^{\mathrm{DM}} = \mathrm{curl}\left(\phi\mathbf{F}^{-1}\right). \tag{72}$$

We note here that the terms involving the velocity gradient came from taking the material time derivative of the area element in the deformed configuration, so these terms correspond to the change in $\boldsymbol{\alpha}^{\mathrm{DM}}$ due to the deforming body itself and not due to dislocation motion. The term on the right-hand side of (72) is responsible for the change in $\boldsymbol{\alpha}^{\mathrm{DM}}$ due to dislocation motion. An expression similar to (72) can be found in Acharya (2004). Eqs. (70) and (72) can be regarded as the transport equations for the two-point tensors $\boldsymbol{\alpha}^{\mathrm{RM}}$ and $\boldsymbol{\alpha}^{\mathrm{DM}}$ written in the referential and spatial frames, respectively.

5. Transport equations for the vector density of dislocations

We now obtain the transport equations for the vector dislocation density fields. To do so, we start by decomposing $\boldsymbol{\alpha}^{\mathrm{RM}}$ into its slip system contribution in terms of the dislocation density vector and the crystal Burgers vectors,

$$\boldsymbol{\alpha}^{\mathrm{RM}}\ = \sum_{l} \boldsymbol{\alpha}^{\mathrm{RM}\ (l)} = \sum_{l} \boldsymbol{\rho}_{\mathrm{R}}^{(l)} \otimes \mathbf{b}_{\mathrm{M}}^{(l)}. \tag{73}$$

Plugging this into the transport Eq. (70) and using (58) for the dislocation current yields

$$\sum_{\mathrm{l}} \dot{\boldsymbol{\rho}}_{\mathrm{R}}^{(l)} \otimes \mathbf{b}_{\mathrm{M}}^{(l)} = \mathrm{Curl}\left(\sum_{l} \mathbf{b}_{\mathrm{M}}^{(l)} \otimes \left(\mathbf{v}_{\mathrm{R}}^{(l)} \times \boldsymbol{\rho}_{\mathrm{R}}^{(l)}\right)\right)\ . \tag{74}$$

Using the curl identity (6) and the fact that $\mathbf{b}_{\mathrm{M}}^{(l)}$ is constant gives

$$\sum_{\mathrm{l}} \dot{\boldsymbol{\rho}}_{\mathrm{R}}^{(l)} \otimes \mathbf{b}_{\mathrm{M}}^{(l)} = \sum_{\mathrm{l}} \mathrm{Curl}\left(\mathbf{v}_{\mathrm{R}}^{(l)} \times \boldsymbol{\rho}_{\mathrm{R}}^{(l)}\right) \otimes\ \mathbf{b}_{\mathrm{M}}^{(l)}. \tag{75}$$

It is now possible to split (75) for the transport equations for individual slip systems

$$\dot{\boldsymbol{\rho}}_{\mathrm{R}}^{(l)} = \mathrm{Curl}\left(\mathbf{v}_{\mathrm{R}}^{(l)} \times \boldsymbol{\rho}_{\mathrm{R}}^{(l)}\right)\ + \dot{\boldsymbol{\rho}}_{\mathrm{R}}^{\mathrm{N}(l)}, \tag{76}$$

where $\dot{\boldsymbol{\rho}}_{\mathrm{R}}^{\mathrm{N}(l)}$ is the rate of network density for slip system l as a result of cross-slip and dislocation junction reactions and annihilation; see Lin and El-Azab (2019) for the case of infinitesimal deformation theory. These rates satisfy the condition: $\sum_{\mathrm{l}} \dot{\boldsymbol{\rho}}_{\mathrm{R}}^{\mathrm{N}(l)} \otimes \mathbf{b}_{\mathrm{M}}^{l} = 0$. We neglect the network terms in this paper by assuming that dislocations on each slip system form their own closed network, and dedicate a future publication to their treatment in the case of finite deformation. In this case, the condition that $\boldsymbol{\alpha}^{\mathrm{RM}\ \mathrm{T}}$ is divergence free leads to

$$\mathrm{Div}\left(\mathbf{b}_{\mathrm{M}}^{(l)} \otimes \boldsymbol{\rho}_{\mathrm{R}}^{(l)}\right) = 0.$$

Using the divergence identity (7) and the fact that $\mathbf{b}_{\mathrm{M}}^{(l)}$ is constant we arrive at,

$$\mathrm{Div}\left(\boldsymbol{\rho}_{\mathrm{R}}^{(l)}\right) = 0. \tag{77}$$

Similarly, we can get transport equations for the vector densities in the current configuration by considering the transport Eq. (72) and decomposing $\boldsymbol{\alpha}^{\mathrm{DM}}$ into slip system contributions,

$$\boldsymbol{\alpha}^{\mathrm{DM}} = \sum_l \boldsymbol{\alpha}^{\mathrm{DM}(l)} = \sum_l \boldsymbol{\rho}_{\mathrm{D}}^{(l)} \otimes \mathbf{b}_{\mathrm{M}}^{(l)}. \tag{78}$$

Substituting this into the transport Eq. (72) gives

$$\sum_l \dot{\boldsymbol{\rho}}_{\mathrm{D}}^{(l)} \otimes \mathbf{b}_{\mathrm{M}}^{(l)} + (\mathrm{tr}(\mathbf{L})\mathbf{I} - \mathbf{L}) \sum_l \boldsymbol{\rho}_{\mathrm{D}}^{(l)} \otimes \mathbf{b}_{\mathrm{M}}^{(l)} = \mathrm{curl}\left(\phi \mathbf{F}^{-1}\right).$$

With the use of (63), this can be rewritten in the form

$$\sum_l \dot{\boldsymbol{\rho}}_{\mathrm{D}}^{(l)} \otimes \mathbf{b}_{\mathrm{M}}^{(l)} + (\mathrm{tr}(\mathbf{L})\mathbf{I} - \mathbf{L}) \sum_l \boldsymbol{\rho}_{\mathrm{D}}^{(l)} \otimes \mathbf{b}_{\mathrm{M}}^{(l)} = \mathrm{curl} \sum_l \mathbf{b}_{\mathrm{M}}^{(l)} \otimes \left(\mathbf{v}_{\mathrm{D}}^{(l)} \times \boldsymbol{\rho}_{\mathrm{D}}^{(l)}\right). \tag{79}$$

Upon using the curl identity (6) and with the addition of network terms, Eq. (79) yields the transport equations for the individual vector densities in the deformed configuration,

$$\dot{\boldsymbol{\rho}}_{\mathrm{D}}^{(l)} + (\mathrm{tr}(\mathbf{L})\mathbf{I} - \mathbf{L})\boldsymbol{\rho}_{\mathrm{D}}^{(l)} = \mathrm{curl}\left(\mathbf{v}_{\mathrm{D}}^{(l)} \times \boldsymbol{\rho}_{\mathrm{D}}^{(l)}\right) + \dot{\boldsymbol{\rho}}_{\mathrm{D}}^{\mathrm{N}(l)}, \tag{80}$$

where, again, a network term is added for completeness.

We remark that the transport equations for the vector densities were derived from the two-point tensors since in these tensors the crystal Burgers vectors in the microstructure configuration are constant. It is also worth noting that these two tensors were considered unimportant by Cermelli and Gurtin (2001) due to the fact that they were not invariant tensors.

Expression (80) is the material form of the transport equation of the density measure in the deformed configuration, $\boldsymbol{\rho}_{\mathrm{D}}$, which can be transformed into a spatial of Eulerian form following the usual techniques of continuum mechanics. In contrast to the two-point dislocation density tensors, the referential and spatial density tensors $\boldsymbol{\alpha}^{\mathrm{R}}$ and $\boldsymbol{\alpha}^{\mathrm{D}}$ have two contributions to their material time derivative, a contribution due to dislocation motion and another due to change in the Burgers vector in the respective configurations. For example, for $\boldsymbol{\alpha}^{\mathrm{D}}$ from (40), the material time derivative is $\dot{\boldsymbol{\alpha}}^{\mathrm{D}} = \dot{\boldsymbol{\rho}}_{\mathrm{D}} \otimes \mathbf{b}_{\mathrm{D}} + \boldsymbol{\rho}_{\mathrm{D}} \otimes \dot{\mathbf{b}}_{\mathrm{D}}$. Because of this, it is not possible to use $\boldsymbol{\alpha}^{\mathrm{D}}$ to isolate an expression for the transport equations for $\boldsymbol{\rho}_{\mathrm{D}}$ because of the additional terms that come from $\dot{\mathbf{b}}_{\mathrm{D}}$. Instead, we start by expanding the material time derivative in (80) into the form

$$\dot{\boldsymbol{\rho}}_{\mathrm{D}}^{(l)} = \boldsymbol{\rho}'^{(l)}_{\mathrm{D}} + \mathrm{grad}\left(\boldsymbol{\rho}_{\mathrm{D}}^{(l)}\right)\mathbf{v}, \tag{81}$$

with the prime denoting the Eulerian time derivative. Using the identity (7) we obtain

$$\mathrm{div}\left(\boldsymbol{\rho}_{\mathrm{D}}^{(l)} \otimes \mathbf{v}\right) = \mathrm{div}(\mathbf{v})\boldsymbol{\rho}_{\mathrm{D}}^{(l)} + \mathrm{grad}\left(\boldsymbol{\rho}_{\mathrm{D}}^{(l)}\right)\mathbf{v},$$

which we write as,

$$\mathrm{div}\left(\boldsymbol{\rho}_{\mathrm{D}}^{(l)} \otimes \mathbf{v}\right) = \mathrm{tr}(\mathrm{L})\boldsymbol{\rho}_{\mathrm{D}}^{(l)} + \mathrm{grad}\left(\boldsymbol{\rho}_{\mathrm{D}}^{(l)}\right)\mathbf{v}. \tag{82}$$

Using the same identity again gives,

$$\mathrm{div}\left(\mathbf{v} \otimes \boldsymbol{\rho}_{\mathrm{D}}^{(l)}\right) = \mathrm{div}\left(\boldsymbol{\rho}_{\mathrm{D}}^{(l)}\right)\mathbf{v} + \mathrm{grad}(\mathbf{v})\boldsymbol{\rho}_{\mathrm{D}}^{(l)}.$$

Neglecting again the network terms and using (77) we write this as

$$\mathrm{div}\left(\mathbf{v} \otimes \boldsymbol{\rho}_{\mathrm{D}}^{(l)}\right) = 0 + \mathbf{L}\boldsymbol{\rho}_{\mathrm{D}}^{(l)}. \tag{83}$$

Looking at just the left-hand side of the transport Eqs. (80) and using (81), we get

$$\dot{\boldsymbol{\rho}}_{\mathrm{D}}^{(l)} + (\mathrm{tr}(\mathbf{L})\mathbf{I} - \mathbf{L})\boldsymbol{\rho}_{\mathrm{D}}^{(l)} = \boldsymbol{\rho}'^{(l)}_{\mathrm{D}} + \mathrm{grad}\left(\boldsymbol{\rho}_{\mathrm{D}}^{(l)}\right)\mathbf{v} + (\mathrm{tr}(\mathbf{L})\mathbf{I} - \mathbf{L})\boldsymbol{\rho}_{\mathrm{D}}^{(l)}.$$

With the use of (82), it becomes: $\boldsymbol{\rho}'^{(l)}_{\mathrm{D}} + \mathrm{div}(\boldsymbol{\rho}_{\mathrm{D}}^{(l)} \otimes \mathbf{v}) - \mathrm{tr}(\mathbf{L})\boldsymbol{\rho}_{\mathrm{D}}^{(l)} + (\mathrm{tr}(\mathbf{L})\mathbf{I} - \mathbf{L})\boldsymbol{\rho}_{\mathrm{D}}^{(l)} = \boldsymbol{\rho}'^{(l)}_{\mathrm{D}} + \mathrm{div}(\boldsymbol{\rho}_{\mathrm{D}}^{(l)} \otimes \mathbf{v}) - \mathbf{L}\rho_{\mathrm{D}}^{(l)}$, and with further use of (83), it becomes: $\boldsymbol{\rho}'^{(l)}_{\mathrm{D}} + \mathrm{div}(\boldsymbol{\rho}_{\mathrm{D}}^{(l)} \otimes \mathbf{v}) - \mathrm{div}(\mathbf{v} \otimes \boldsymbol{\rho}_{\mathrm{D}}^{(l)})$. Finally, using (8), it can be simplified to: $\boldsymbol{\rho}'^{(l)}_{\mathrm{D}} - \mathrm{curl}(\mathbf{v} \times \boldsymbol{\rho}_{\mathrm{D}}^{(l)})$. The final form for the transport equations for the vector densities in the deformed configuration then becomes

$$\boldsymbol{\rho}'^{(l)}_{\mathrm{D}} = \mathrm{curl}\left((\mathbf{v}_{\mathbf{D}}^{(l)} + \mathbf{v}) \times \boldsymbol{\rho}_{\mathrm{D}}^{(l)}\right) + \boldsymbol{\rho}'^{\mathrm{N}(l)}_{\mathrm{D}}, \tag{84}$$

where the network term was added. This equation represents the transport of dislocations in the deformed configuration and the velocity term $(\mathbf{v}_{\mathrm{D}}^{(l)} + \mathbf{v})$ can be thought of as the absolute velocity of dislocations, which is the sum of dislocation velocity relative to the crystal, $\mathbf{v}_{\mathrm{D}}^{(l)}$, and the crystal velocity, $\mathbf{v}$. A condition similar to (77) does apply to the spatial density $\boldsymbol{\rho}_{\mathrm{D}}^{(l)}$. Again, we hold off on the analysis of the network terms $\boldsymbol{\rho}_{\mathrm{D}}^{\mathrm{N}(l)}$ for a future publication.

We can now move on to deriving the driving forces associated with referential and spatial forms (76) and (84) of the transport equations for the vector density of dislocations. For completeness, thought, we refer the reader to Appendix A where the transport relations for the remaining dislocation density tensors, namely, $\boldsymbol{\alpha}^{\mathrm{R}}$, $\boldsymbol{\alpha}^{\mathrm{M}}$, and $\boldsymbol{\alpha}^{\mathrm{D}}$, are derived.

6. Crystal kinetics and constitutive analysis

We now wish to connect the velocity of dislocations to the corresponding driving force. We do so by deriving the force conjugate to the velocity of dislocations, from which the velocities can be fixed using a mobility law.

We begin by introducing the stress equilibrium equations. Neglecting inertia, Cauchy stress, $\boldsymbol{\sigma}$, satisfies the static equilibrium equation with no body forces in the deformed configuration,

$$\mathrm{div}(\boldsymbol{\sigma}) = 0. \tag{85}$$

In the reference configuration equilibrium takes on the form,

$$\mathrm{Div}\left(\mathbf{P}^{\mathrm{T}}\right) = 0, \tag{86}$$

where $\mathbf{P}$ is the first Piola–Kirchhoff (PK1) stress tensor, which measures the traction in the deformed configuration on an area element in the reference configuration. It is related to the second Piola–Kirchhoff (PK2) stress tensor, $\mathbf{S}$, by $\mathbf{P}^{\mathrm{T}} = \mathbf{S}^{\mathrm{T}}\mathbf{F}^{\mathrm{T}}$.

6.1. Power of deformation in reference configuration

The power of deformation in the deformed configuration is $\boldsymbol{\sigma} : \mathbf{D}$, with $\mathbf{D}$ being the symmetric part of the velocity gradient, or the rate-of-strain tensor. This power can be pulled back to give its counterpart in the reference configuration: $\mathrm{J}\boldsymbol{\sigma} : \mathbf{D}$. By further using $\mathbf{D} = \mathbf{F}^{-1}\dot{\mathbf{E}}\mathbf{F}^{-T}$ and using the relationships between Cauchy stress and the second Piola–Kirchhoff stress, the referential power density can be written in the form:

$$\mathrm{J}(\boldsymbol{\sigma} : \mathbf{D}) = \mathbf{S} : \dot{\mathbf{E}}. \tag{87}$$

Below we show that the power of deformation in the reference configuration can be split into two contributions associated with the dislocation motion and elastic strain rate. By exploiting Eq. (20) for the Lagrangian strain, we can write:

$$\mathbf{S} : \dot{\mathbf{E}} = \mathbf{S} : \left(\dot{\overline{\mathbf{F}^{\mathrm{pT}}\mathbf{E}^{\mathrm{e}}\mathbf{F}^{\mathrm{p}}}}\right) + \mathbf{S} : \dot{\mathbf{E}}^{\mathrm{p}}, \tag{88}$$

which simplifies to

$$\mathbf{S} : \dot{\mathbf{E}} = \mathbf{M} : \left(\mathbf{F}^{\mathrm{p}-1}\phi\right) + \mathbf{S} : \left(\mathbf{F}^{\mathrm{pT}}\dot{\mathbf{E}}^{\mathrm{e}}\mathbf{F}^{\mathrm{p}}\right), \tag{89}$$

with $\mathbf{M} = \mathbf{CS}$ being the referential Mandel stress. We refer the reader to Appendix B for the algebra used to rewrite Eq. (88) into (89). We note that the quantity $\mathbf{S} : \dot{\mathbf{E}}$ is comprised of a term associated with the motion of dislocations, $\mathbf{M} : (\mathbf{F}^{p-1}\phi)$, and another corresponding to the elastic energy storage, $\mathbf{S} : (\mathbf{F}^{\mathrm{pT}}\dot{\mathbf{E}}^{\mathrm{e}}\mathbf{F}^{\mathrm{p}})$.

6.2. Constitutive analysis

In this section, we derive the elastic and plastic constitutive relationships from the principles of thermodynamics. As expected, the elastic constitutive relationship corresponds to that of a hyperelastic solid. The plastic counterpart is associated with dissipation due to dislocation motion and it leads to defining the configurational force acting on dislocations in the reference configuration, which is the Peach–Koehler force in a finite-deformation setting. To achieve this goal, we start with the global referential free energy imbalance ignoring entropic effects,

$$\int \left(\dot{\psi}_R - \mathbf{S} : \dot{\mathbf{E}}\right)\mathrm{dV}_{\mathrm{R}} \leq 0, \tag{90}$$

with ψ_{R} being the referential free energy density. We assume that the free energy can be split into contributions, the stored elastic energy plus a second part due to dislocations (Hochrainer, 2016),

$$\psi_{\mathrm{R}} = \psi_{\mathrm{R}}^{\mathrm{e}} + \psi_{\mathrm{R}}^{\mathrm{p}}. \tag{91}$$

For a technical reason that will become clear later, the deformed free energy density counterparts, ψ_{D}, $\psi_{\mathrm{D}}^{\mathrm{e}}$ and $\psi_{\mathrm{D}}^{\mathrm{p}}$, are defined per unit mass. We expect these scalars to transform according to,

$$\begin{aligned} \psi_{\mathrm{R}}^{\mathrm{e}} &= \rho_{\mathrm{R}}\psi_{\mathrm{D}}^{\mathrm{e}} \\ \psi_{\mathrm{R}}^{\mathrm{p}} &= \rho_{\mathrm{R}}\psi_{\mathrm{D}}^{\mathrm{p}}. \end{aligned} \tag{92}$$

We consider writing (91) in an equivalent form,

$$\psi_{\mathrm{R}} = \rho_{\mathrm{R}}\psi_{\mathrm{D}}^{\mathrm{e}} + \psi_{\mathrm{R}}^{\mathrm{p}}. \tag{93}$$

Since the referential density does not depend on time, we write the free energy imbalance as (Gurtin et al., 2010),

$$\int \left(\rho_{\mathrm{R}}\dot{\psi}^{\mathrm{e}}_{\mathrm{D}} + \dot{\psi}^{\mathrm{p}}_{\mathrm{P}} - \mathbf{S} : \dot{\mathbf{E}}\right)\mathrm{dV_R} \le 0. \tag{94}$$

Let us assume that the elastic and defect free energy contributions in the deformed configuration have the form,

$$\begin{aligned}\psi^{\mathrm{e}}_{\mathrm{D}} &= \hat{\psi}^{\mathrm{e}}_{\mathrm{D}}\left(\mathbf{F^e}\right)\\ \psi^{\mathrm{p}}_{\mathrm{R}} &= \hat{\psi}^{\mathrm{p}}_{\mathrm{R}}\left(\boldsymbol{\rho}^{(l)}_{\mathrm{R}}\right).\end{aligned} \tag{95}$$

Upon using the chain rule of differentiation with respect to time, (95) gives

$$\begin{aligned}\dot{\psi}^{\mathrm{e}}_{\mathrm{D}} &= \frac{\partial\hat{\psi}^{\mathrm{e}}_{\mathrm{D}}}{\partial\mathbf{F^e}} : \dot{\mathbf{F}}^{\mathbf{e}}\\ \dot{\psi}^{\mathrm{p}}_{\mathrm{P}} &= \sum\nolimits_{l} \frac{\partial\hat{\psi}^{\mathrm{p}}_{\mathrm{R}}}{\partial\boldsymbol{\rho}^{(l)}_{\mathrm{R}}} \cdot \dot{\boldsymbol{\rho}}^{(l)}_{R}.\end{aligned} \tag{96}$$

Plugging this into the free energy imbalance equation yields

$$\int \left(\rho_{\mathrm{R}}\frac{\partial\hat{\psi}^{\mathrm{e}}_{\mathrm{D}}}{\partial\mathbf{F^e}} : \dot{\mathbf{F}}^{\mathbf{e}} - \mathbf{S} : \dot{\mathbf{E}} + \sum_{l}\frac{\partial\hat{\psi}^{\mathrm{p}}_{\mathrm{R}}}{\partial\boldsymbol{\rho}^{(l)}_{\mathrm{R}}} \cdot \dot{\boldsymbol{\rho}}^{(l)}_{R}\right)\mathrm{dV_R} \le 0. \tag{97}$$

From (89) we can write the free energy imbalance as

$$\int \left(\rho_{\mathrm{R}}\frac{\partial\hat{\psi}^{\mathrm{e}}_{\mathrm{D}}}{\partial\mathbf{F^e}} : \dot{\mathbf{F}}^{\mathbf{e}} - \mathbf{S} : \left(\mathbf{F^{pT}}\dot{\mathbf{E}}^{\mathbf{e}}\mathbf{F^p}\right)\right)\mathrm{dV_R} + \int \left(\sum_{l}\frac{\partial\hat{\psi}^{\mathrm{p}}_{\mathrm{R}}}{\partial\boldsymbol{\rho}^{(l)}_{\mathrm{R}}} \cdot \dot{\boldsymbol{\rho}}^{(l)}_{R} - \mathbf{M} : \left(\mathbf{F}^{\mathrm{p}-1}\phi\right)\right)\mathrm{dV_R} \le 0, \tag{98}$$

where we have grouped the terms according to corresponding rate quantities. We further simplify this inequality below to obtain the hyperelastic constitutive relationship and the driving force for dislocation motion.

6.2.1. Elastic constitutive response of the crystal

Let us call the integrals in (98) the elastic and plastic terms, respectively. Our strategy now is to write the expression $\mathbf{S} : (\mathbf{F^{pT}}\dot{\mathbf{E}}^{\mathbf{e}}\mathbf{F^p})$ under the first integral in terms of the rate of the elastic distortion so that we can group it with the first term. To this end, using properties of the double inner product we can write

$$\mathbf{S} : \left(\mathbf{F}^{\mathrm{pT}}\dot{\mathbf{E}}^{\mathrm{e}}\mathbf{F}^{\mathrm{p}}\right) = \left(\mathbf{F}^{\mathrm{p}}\mathbf{S}\mathbf{F}^{\mathrm{pT}}\right) : \dot{\mathbf{E}}^{\mathrm{e}}. \tag{99}$$

Since $(\mathbf{F^p}\mathbf{S}\mathbf{F^{pT}})$ is symmetric it is possible to express this in the form

$$\left(\mathbf{F}^{\mathrm{p}}\mathbf{S}\mathbf{F}^{\mathrm{pT}}\right) : \dot{\mathbf{E}}^{\mathrm{e}} = \left(\mathbf{F}^{\mathrm{p}}\mathbf{S}\mathbf{F}^{\mathrm{pT}}\right) : \left(\mathbf{F}^{\mathrm{eT}}\dot{\mathbf{E}}^{\mathrm{e}}\right). \tag{100}$$

Using the double inner product properties again gives

$$\left(\mathbf{F}^{\mathrm{p}}\mathbf{S}\mathbf{F}^{\mathrm{pT}}\right) : \dot{\mathbf{E}}^{\mathrm{e}} = \left(\mathbf{F}^{\mathrm{e}}\mathbf{F}^{\mathrm{p}}\mathbf{S}\mathbf{F}^{\mathrm{pT}}\right) : \dot{\mathbf{E}}^{\mathrm{e}}. \tag{101}$$

With this, the elastic integral in the free energy imbalance (97) becomes

$$\int \left(\rho_{\mathrm{R}}\frac{\partial\hat{\psi}^{\mathrm{e}}_{\mathrm{D}}}{\partial\mathbf{F^e}} - \mathbf{F}^{\mathrm{e}}\mathbf{F}^{\mathrm{p}}\mathbf{S}\mathbf{F}^{\mathrm{pT}}\right) : \dot{\mathbf{F}}^{\mathbf{e}}\mathrm{dV_R}. \tag{102}$$

For arbitrary motion of the body and due to the non-dissipative nature of this term we require the integrand to vanish

$$\rho_{\mathrm{R}}\frac{\partial\hat{\psi}^{\mathrm{e}}_{\mathrm{D}}}{\partial\mathbf{F^e}} - \mathbf{F}^{\mathrm{e}}\mathbf{F}^{\mathrm{p}}\mathbf{S}\mathbf{F}^{\mathrm{pT}} = 0. \tag{103}$$

Solving (102) for the PK2 stress gives

$$\mathbf{S} = \mathbf{F}^{p-1}\left(\mathbf{F}^{e-1}\rho_{\mathrm{R}}\frac{\partial\hat{\psi}^{\mathrm{e}}_{\mathrm{D}}}{\partial\mathbf{F^e}}\right)\mathbf{F}^{p-T}. \tag{104}$$

We can now start to talk about elastic materials in this context. If we define the PK1 stress in the microstructure space as,

$$\mathbf{P^e} \equiv \rho_{\mathrm{M}}\frac{\partial\hat{\psi}^{\mathrm{e}}_{\mathrm{D}}}{\partial\mathbf{F^e}}. \tag{105}$$

Assuming there exists a mass density such that $\mathrm{J}^{\mathrm{p}}\rho_{\mathrm{M}}=\rho_{\mathrm{R}}$, then by using the transformation relation for the stresses we obtain $\mathbf{S}=\mathrm{J}^{\mathrm{p}}\mathbf{F}^{-1}\mathbf{P}^{\mathrm{e}}\mathbf{F}^{p-T}=\mathrm{J}^{\mathrm{p}}\mathbf{F}^{-1}\rho_{\mathrm{M}}\frac{\partial\hat{\psi}_{\mathrm{D}}^{\mathrm{e}}}{\partial\mathbf{F^{e}}}\mathbf{F}^{p-T}=\mathbf{F}^{p-1}(\mathbf{F}^{e-1}\rho_{\mathrm{R}}\frac{\partial\hat{\psi}_{\mathrm{D}}^{\mathrm{e}}}{\partial\mathbf{F^{e}}})\mathbf{F}^{p-T}$, which corresponds to the constitutive requirement (104). Using the transformation between the PK2 and Cauchy stress yields

$$\boldsymbol{\sigma}=\rho_{\mathrm{D}}\frac{\partial\hat{\psi}_{\mathrm{D}}^{\mathrm{e}}}{\partial\mathbf{F^{e}}}\mathbf{F}^{\mathrm{eT}},\tag{106}$$

with $\rho_{\mathrm{D}}=J^{-1}\rho_{\mathrm{R}}$ is the mass density in the deformed configuration. The relationship (106) is the reminiscent of the standard constitutive law for a hyperelastic solid (Gurtin et al., 2010).

6.2.2. The force acting on dislocations and mobility law

We next consider the plastic integral in free energy imbalance (98), which is related to the dislocation transport. We want to manipulate these terms so that we get an expression that looks like $\mathbf{v}_{\mathbf{R}}^{l}\cdot(-\mathbf{f})\leq 0$, where $\mathbf{f}$ is a force that is rate-of-work conjugate to the dislocation velocity field. Once we have this expression, we can write a velocity mobility law in the form: $\mathbf{v}_{\mathbf{R}}^{l}=\mathbf{v}_{\mathbf{R}}^{l}(\mathbf{f})$. To this end we consider the term $\mathbf{M}:(\mathbf{F^{p}}^{-1}\phi)$,

$$\begin{aligned}\mathbf{M}:\left(\mathbf{F^{p}}^{-1}\phi\right)&=\mathbf{M}:\sum_{l}\mathbf{F^{p}}^{-1}\mathbf{b}_{\mathrm{M}}^{(l)}\otimes\left(\mathbf{v}_{\mathrm{R}}^{(l)}\times\boldsymbol{\rho}_{\mathrm{R}}^{(l)}\right)\\&=\sum_{l}\mathbf{b}_{\mathrm{R}}^{(l)}\otimes\left(\mathbf{v}_{\mathrm{R}}^{(l)}\times\boldsymbol{\rho}_{\mathrm{R}}^{(l)}\right)=\sum_{l}\mathbf{M}:\mathbf{b}_{\mathrm{R}}^{(l)}\otimes\left(\mathbf{v}_{\mathrm{R}}^{(l)}\times\boldsymbol{\rho}_{\mathrm{R}}^{(l)}\right)\\&=\sum_{l}M_{ij}b_{\mathrm{R}\ i}^{(l)}\epsilon_{kmj}v_{\mathrm{R}\ k}^{(l)}\rho_{\mathrm{R}\ m}^{(l)}=\sum_{l}v_{\mathrm{R}\ k}^{(l)}\epsilon_{kmj}M_{ij}b_{\mathrm{R}\ i}^{(l)}\rho_{\mathrm{R}\ m}^{(l)}\end{aligned}$$

Since $\epsilon_{kmj}=\epsilon_{jmk}$, we can write, $\sum_{l}v_{\mathrm{R}\ k}^{(l)}\epsilon_{jmk}M_{ij}b_{\mathrm{R}\ i}^{(l)}\rho_{\mathrm{R}\ m}^{(l)}=\sum_{l}\mathbf{v}_{\mathrm{R}}^{(l)}\cdot(\mathbf{M}\mathbf{b}_{\mathrm{R}}^{(l)}\times\boldsymbol{\rho}_{\mathrm{R}}^{(l)})$. This yields a simplified expression for the $\mathbf{M}:(\mathbf{F^{p}}^{-1}\phi)$ as follows:

$$\mathbf{M}:\left(\mathbf{F^{p}}^{-1}\phi\right)=\sum_{l}\mathbf{v}_{\mathrm{R}}^{(l)}\cdot\left(\left(\mathbf{b}_{\mathrm{R}}^{(l)}\cdot\mathbf{M}^{\mathrm{T}}\right)\times\boldsymbol{\rho}_{\mathrm{R}}^{(l)}\right).\tag{107}$$

We will now look at the term $\sum_{l}\rho_{\mathrm{R}}\frac{\partial\widehat{\psi}}{\partial\rho_{\mathrm{R}}^{l}}\cdot\dot{\boldsymbol{\rho}}_{R}^{(l)}$. We manipulate this term by borrowing the expression for $\dot{\boldsymbol{\rho}}_{R}^{(l)}$ from the transport Eq. (76) while ignoring the network term for simplicity. Prior to inserting the corresponding expression, we manipulate it further by replacing the curl operator with the divergence operator as follows:

$$\mathrm{Curl}\left(\mathbf{v}_{\mathrm{R}}^{(l)}\times\boldsymbol{\rho}_{\mathrm{R}}^{(l)}\right)=\mathrm{Div}\left(\mathbf{v}_{\mathrm{R}}^{(l)}\otimes\boldsymbol{\rho}_{\mathrm{R}}^{(l)}-\boldsymbol{\rho}_{\mathrm{R}}^{(l)}\otimes\mathbf{v}_{\mathrm{R}}^{(l)}\right).$$

With this, the corresponding term in the free energy imbalance becomes

$$\int\sum_{l}\frac{\partial\hat{\psi}_{\mathrm{R}}^{\mathrm{p}}}{\partial\boldsymbol{\rho}_{\mathrm{R}}^{(l)}}\cdot\mathrm{Div}\left(\mathbf{v}_{\mathrm{R}}^{(l)}\otimes\boldsymbol{\rho}_{\mathrm{R}}^{(l)}-\boldsymbol{\rho}_{\mathrm{R}}^{(l)}\otimes\mathbf{v}_{\mathrm{R}}^{(l)}\right)\mathrm{dV}_{\mathrm{R}}.\tag{108}$$

Carrying out integration by parts, with periodic boundary conditions to get rid of surface terms, the last integral can be expressed in the form

$$-\int\sum_{l}\mathrm{Grad}\left(\frac{\partial\hat{\psi}_{\mathrm{R}}^{\mathrm{p}}}{\partial\boldsymbol{\rho}_{\mathrm{R}}^{(l)}}\right):\left(\mathbf{v}_{\mathrm{R}}^{(l)}\otimes\boldsymbol{\rho}_{\mathrm{R}}^{(l)}-\boldsymbol{\rho}_{\mathrm{R}}^{(l)}\otimes\mathbf{v}_{\mathrm{R}}^{(l)}\right)\mathrm{dV}_{\mathrm{R}}.\tag{109}$$

which can be further simplified to

$$-\int\sum_{l}\mathbf{v}_{\mathrm{R}}^{(l)}\cdot\left[\left(\mathbf{A}^{(l)}-\mathbf{A}^{(l)\mathrm{T}}\right)\boldsymbol{\rho}_{\mathrm{R}}^{(l)}\right]\mathrm{dV}_{\mathrm{R}},\tag{110}$$

with $\mathbf{A}^{(l)}\equiv\mathrm{Grad}(\frac{\partial\hat{\psi}_{\mathrm{R}}^{\mathrm{p}}}{\partial\boldsymbol{\rho}_{\mathrm{R}}^{(l)}})$. Since $(\mathbf{A}^{(l)}-\mathbf{A}^{(l)\mathrm{T}})$ is antisymmetric, it has an axial vector $\boldsymbol{\omega}^{(l)}$ defined such that $(\mathbf{A}^{(l)}-\mathbf{A}^{(l)\mathrm{T}})\,\boldsymbol{\xi}_{\mathrm{R}}^{(l)}=\boldsymbol{\omega}^{(l)}\times\boldsymbol{\xi}_{\mathrm{R}}^{(l)}$ and given by $\omega_{i}^{(l)}=-\frac{1}{2}\epsilon_{ijk}(\boldsymbol{A}^{(l)}-\boldsymbol{A}^{(l)\mathrm{T}})_{jk}$. This axial vector can also be expressed in the form: $\boldsymbol{\omega}^{(l)}=\mathrm{Curl}(\frac{\partial\hat{\psi}_{\mathrm{R}}^{\mathrm{p}}}{\partial\rho_{\mathrm{R}}^{(l)}})$. With this, Eq. (110) becomes,

$$\int\sum_{l}\frac{\partial\hat{\psi}_{\mathrm{R}}^{\mathrm{p}}}{\partial\boldsymbol{\rho}_{\mathrm{R}}^{(l)}}\cdot\dot{\boldsymbol{\rho}}_{R}^{(l)}\mathrm{dV}_{\mathrm{R}}=-\int\sum_{l}\rho_{\mathrm{R}}^{(l)}\mathbf{v}_{\mathrm{R}}^{(l)}\cdot\left[\mathrm{Curl}\left(\frac{\partial\hat{\psi}_{\mathrm{R}}^{\mathrm{p}}}{\partial\boldsymbol{\rho}_{\mathrm{R}}^{(l)}}\right)\times\boldsymbol{\xi}_{\mathrm{R}}^{(l)}\right]\mathrm{dV}_{\mathrm{R}},\tag{111}$$

where $\boldsymbol{\rho}_{\mathrm{R}}^{(l)}=\rho_{\mathrm{R}}^{(l)}\boldsymbol{\xi}_{\mathrm{R}}^{(l)}$. Adding the simplified terms (107) and (111), the second integral in Eq. (97) becomes

$$\int\sum_{l}\rho_{\mathrm{R}}^{(l)}\mathbf{v}_{\mathrm{R}}^{(l)}\cdot\left[-\left(\mathbf{b}_{\mathrm{R}}^{(l)}\cdot\mathbf{M}^{\mathrm{T}}+\boldsymbol{\omega}^{(l)}\right)\times\boldsymbol{\xi}_{\mathrm{R}}^{(l)}\right]\mathrm{dV}_{\mathrm{R}}\leq 0.\tag{112}$$

The quantity between brackets is nothing but the configuration force acting on dislocations. It has the proper dimensions of force per unit length, and the multiplication by the scalar density of dislocation and the velocity yields the contribution to the rate of decline of the free energy per unit volume, with the minus sign taken into consideration. We note here that a similar expression for the driving force for dislocations in the reference configuration was given in Po et al. (2019) where the Mandel stress is used as a driving force with an additional back stress term coming from the free energy. We may thus define the referential Peach–Koehler force in the case of finite deformation by

$$\mathbf{f}_{\mathrm{R}}^{(l)} = \left(\mathbf{b}_{\mathbf{R}}^{(l)} \cdot \mathbf{M}^{\mathrm{T}} + \boldsymbol{\omega}^{(l)}\right) \times \boldsymbol{\xi}_{\mathrm{R}}^{(l)}. \tag{113}$$

A similar procedure can be used to obtain the Peach-Kohler force in the deformed configuration by considering the free energy imbalance in that configuration; this results in the usual expression for the driving force with the Cauchy stress as the driving stress measure

$$\mathbf{f}_{\mathrm{D}}^{(l)} = \left(\mathbf{b}_{\mathrm{D}}^{(l)} \cdot \boldsymbol{\sigma}^{\mathrm{T}} + \boldsymbol{\omega}_{\mathrm{D}}^{(l)}\right) \times \boldsymbol{\xi}_{\mathrm{D}}^{(l)}, \tag{114}$$

where $\boldsymbol{\omega}_{\mathrm{D}}^{(l)} \equiv \mathrm{curl}(\frac{\partial \hat{\psi}_{\mathrm{D}}^{\mathrm{p}}}{\partial \boldsymbol{\rho}_{\mathrm{D}}^{(l)}})$. The reader is referred to Appendix C for relevant details of the derivation. Because the integral in (112) is negative, a mobility law can then be postulated to yield the dislocation velocity in terms of the driving force. The simplest form of such a law is

$$\mathbf{v}_{\mathrm{R}}^{(l)} = M\mathbf{f}_{\mathrm{R}}^{(l)}, \tag{115}$$

with M being a positive quantity. Regardless of its form, such a mobility law connects the dislocation velocity to the local stress state and closes the set of equations to be solved once a constitutive function $\psi_{\mathrm{R}}^{\mathrm{p}} = \hat{\psi}_{\mathrm{R}}^{\mathrm{p}}(\boldsymbol{\rho}_{\mathrm{R}}^{l})$ is fixed. These equations are:

$$\begin{cases} \mathrm{Div}\left(\mathbf{P}^{\mathrm{T}}\right) = 0 \\ \dot{\boldsymbol{\rho}}_{\mathrm{R}}^{(l)} = \mathrm{Curl}\left(\mathbf{v}_{\mathrm{R}}^{(l)} \times \boldsymbol{\rho}_{\mathrm{R}}^{(l)}\right) + \dot{\boldsymbol{\rho}}_{\mathrm{R}}^{\mathrm{N}(l)} \\ \mathbf{v}_{\mathrm{R}}^{(l)} = \mathrm{M}\mathbf{f}_{\mathrm{R}}^{(\boldsymbol{l})}. \end{cases} \tag{116}$$

where the network contribution to the rate of change of the slip system density $\dot{\boldsymbol{\rho}}_{\mathrm{R}}^{(l)}$ has been restored. The numerical treatment of these equations fully coupled with the rest of the equations of finite-deformation crystal mechanics will be the subject of a forthcoming publication. Only a few static solution problems, i.e., when $\mathbf{v}_{\mathrm{R}}^{(l)} = 0$, are presented in the next section to illustrate some of the important relationships.

We remark here that, in the development presented so far the idea of an arbitrary reference configuration is important, and we refer the reader to Appendix D where an attempt is made at defining what this should mean in the case of dislocated crystals.

7. Static solutions and discussion

In this section, numerical solutions are presented for a set of finite-eigenstrain problem involving the introduction of plastic distortion into a single crystal and the calculation of the dislocation and elastic fields. The calculations are done for FCC iron with shear modulus of 79.52 GPa, Poisson's ratio of 0.2945, and Burgers vector of 0.254 nm Reed and Clark, 1983). The domain size was 5 μm on the edge. The governing equations are solved using a total Lagrangian approach with the plastic distortion specified that corresponds to simple static dislocations arrays. A linear elastic constitutive law for ((105) is assumed with an elastic tensor being isotropic. Periodic boundary conditions are assumed throughout and no external loads are present. Details of the numerical solution scheme will appear in a future publication.

The first problem is one in which plastic distortion is introduced so as to correspond to a dislocation bundle in the form of a loop. A small plastic distortion is introduced first to enable comparison with the linearized (infinitesimal) eigenstrain problems, then a finite distortion is introduced to check the differences in the elastic fields between the two cases. The situation is illustrated in Fig. 2. The plastic distortion is smeared so as to correspond to a dislocation bundle that has a density of a Gaussian profile in both the radial and z directions. The stress field is plotted in Fig. 3 in the deformed configuration for the case of small strain along with the analytical solution reported in Langdon (2000) for a loop embedded in an infinite domain. The comparison thus makes sense near the dislocation bundle and away from the domain boundary. The solution shows that the stress contours are equivalent. Good agreement of the solution near the dislocation loops, which is dominated by the singular field, is clear in Fig. 3.

Next, we consider a denser distribution of dislocations obtained by increasing the magnitude of the plastic distortion introduced into the domain of solution. In this case, the lattice rotation effects start to become significant. The plastic distortion is shown in Fig. 4. And the resulting Cauchy stress field is shown in Fig. 5 along with the solution produced in Langdon (2000) for the linear elastic solution case. The figure shows that there is some rotation of the contours in the case of finite deformation (top panels). This rotation becomes more prominent when larger localized dislocation densities are introduced as the magnitude of the plastic distortion is increased.

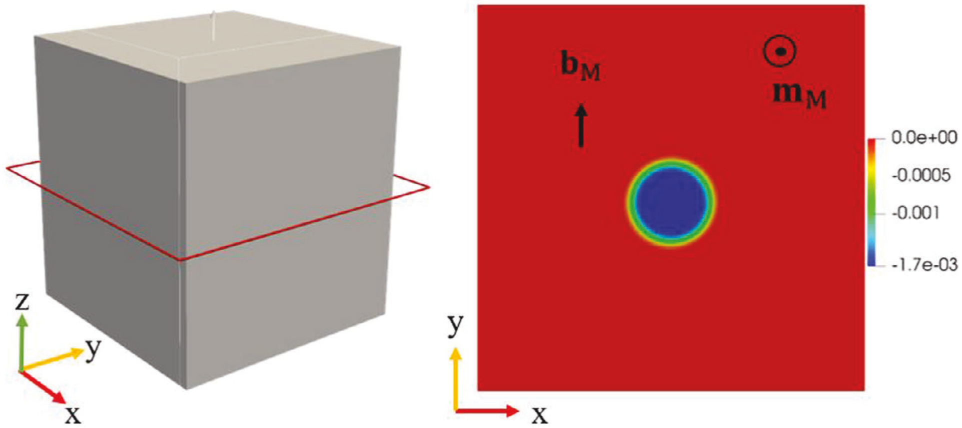

Fig. 2. A 3D depiction of the simulation domain is shown to the left with a red plane intersecting it corresponding to the slip plan to the right, with the plastic slip field, γ, introduced parallel to the x-y plane and represented by colors. Burgers vector is oriented along the y direction and slip normal, $\mathbf{m}_M$, in the z direction. (For interpretation of the references to color in this figure legend, the reader is referred to the web version of this article.)

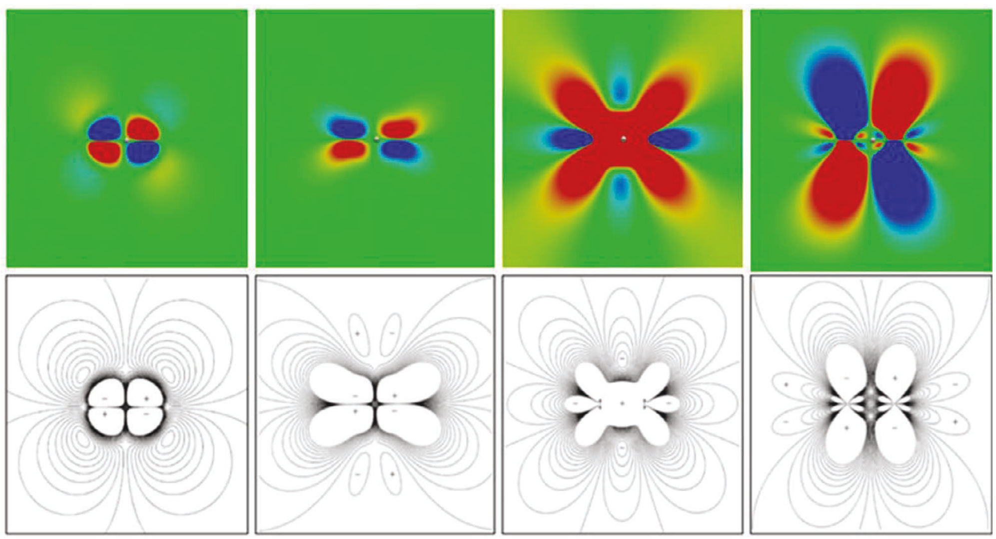

Fig. 3. Cauchy stress in the y-z plane passing through the middle of the domain of solution. From the left to right the components are σ_{11}, σ_{22}, σ_{23} and σ_{33}. The top panels are obtained by our solution method (with red and blue colors representing positive and negative stresses) and the lower panels represent the analytical solution of a dislocation loop in an infinite medium reported in (Langdon, 2000). (For interpretation of the references to color in this figure legend, the reader is referred to the web version of this article.)

In this next test problem, we consider a plastic distortion giving rise to tilt boundaries. The tilt boundaries consist of vertical arrays of edge dislocations generated by uniform plastic slip of 4% in the channel between the boundaries. The termination of slip at the boundaries with sharp gradients creates the dislocation arrays. This situation is depicted in Fig. 6. The non-trivial component of the referential dislocation density tensor associated with the tilt boundaries is α^{R}_{12}. This component is shown in Fig. 7. The dislocation lines run along the x direction for positive dislocations and along the negative x direction for negative dislocations, with the crystallographic Burgers vector (the direction of slip) pointing in the y direction. The magnitude of the plastic distortion and its gradient at the channel ends fully fix the values of α^{R}_{12}.

We now illustrate the effect of lattice rotation on the dislocation density measure by investigating the density tensor in the deformed configuration for the tilt boundary case discussed above. The non-zero components of the tensor are α^{D}_{12} and α^{D}_{13}, with the latter component arising due to the elastic lattice rotation of the microstructure Burgers vector. Both components are shown in Fig. 8. As clear from the figure, the rotation effects are non-negligible.

To quantify the elastic lattice rotation further, we calculate that quantity in terms of a rotation vector $\boldsymbol{\theta} = \theta\mathbf{w}$, with θ being the magnitude of rotation about axis $\mathbf{w}$ (Larson et al., 2007). The vector $\boldsymbol{\theta}$ is related to the pure rotation part $\mathbf{R}^{e}$ of the elastic distortion $\mathbf{F}^{e}$ via

$$\mathbf{R}^{e} = \exp(\mathbf{W}) = \cos(\theta)\mathbf{I} + \sin(\theta)(\mathbf{w}\times) + (1 - \cos(\theta))\mathbf{w} \otimes \mathbf{w}, \tag{117}$$

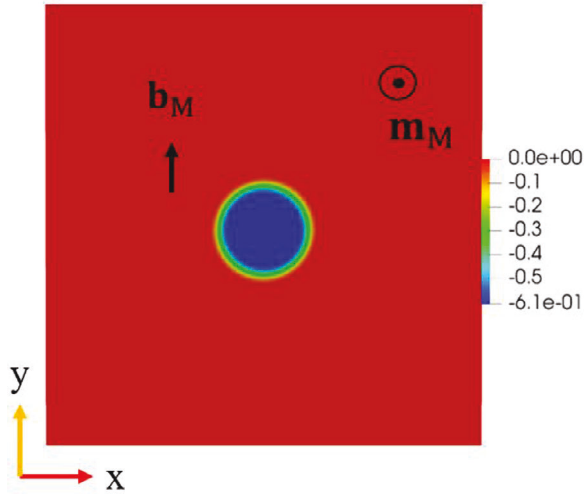

Fig. 4. A finite plastic shear that is more than two orders of magnitude larger than that shown in Fig. 2. A finite-deformation solution of the eigenstrain problem is required in this case.

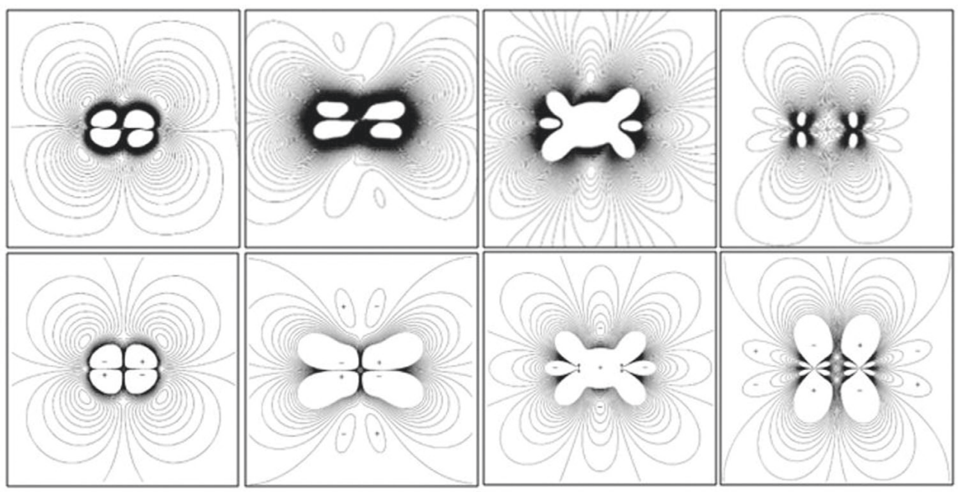

Fig. 5. Cauchy stress corresponding to the finite plastic slip shown in Fig. 4, plotted in the deformed configuration on a y-z plane passing through the middle of the solution domain (Fig. 2). The top panels show our solution and the lower panels represent the analytical solution for a single dislocation loop in an infinite domain (Langdon, 2000). From the left to right the components are $\sigma_{11}, \sigma_{22}, \sigma_{23}$ and σ_{33}. The signs of our solution match the analytical result.

where $\mathbf{W} = (\boldsymbol{\theta}\times)$ is an anti-symmetric second order tensor with $\boldsymbol{\theta}$ as its axial vector, and the polar decomposition $\mathbf{F}^e = \mathbf{R}^e\mathbf{U}^e$ holds with $\mathbf{U}^e$ being the right stretch tensor. In the current case, $\mathbf{F}^e$ is found from $\mathbf{F}^e = \mathbf{F}\mathbf{F}^{p-1}$, where $\mathbf{F}^p$ is prescribed and $\mathbf{F}$ is found from the solution of the problem. Once the elastic distortion is known the rotation vector can be solved for using (119), which is trivial in 2D situations as in the tilt walls example discussed earlier. A line profile of the rotation angle θ is plotted along the y coordinate in Fig. 9. We see that the lattice is initially rotated slightly then at the first tilt boundary we get jump in the rotation angle due to the elastic strains from the dislocations and another jump in the opposite direction at the next tilt boundary, resulting in a rotation angle which is periodic.

Finally, we compare Cauchy and Mandel stresses in Fig. 10 to show the similarities and differences in the forces that drive dislocation motion in the deformed and reference configurations. Cauchy stress to the left would be the stress driving dislocation motion in the deformed configuration, while the Mandel stress will do the same in the reference configuration. The magnitudes and distributions of the two stress measures are similar for this test case with the only minor difference being the 22 stress components at the tilt boundary. For larger elastic strains though these measures become increasingly different in the 32 and 22 components which is not shown here. An extra stress component is plotted for the Mandel stress to show that it is nearly symmetric for this magnitude of deformation used in this example.

The simulated configuration of two tilt boundaries with opposite signs was inspired by the general experimental observation of alternating signs of neighboring boundaries, which prevents the buildup of large orientation gradients in the center

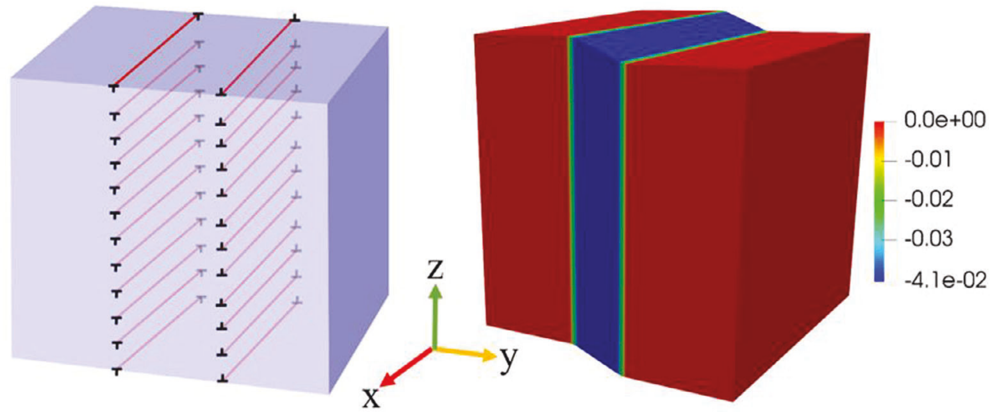

Fig. 6. A discrete representation of the two tilt boundaries (left), with two vertical arrays of negative and positive edge dislocations forming the two boundaries. A uniform plastic slip of 4% was introduced in the channel between the boundaries, with sharp gradients giving rise to the dislocation arrays. The plastic slip is plotted to the right on the deformed configuration associated with the two tilt boundaries.

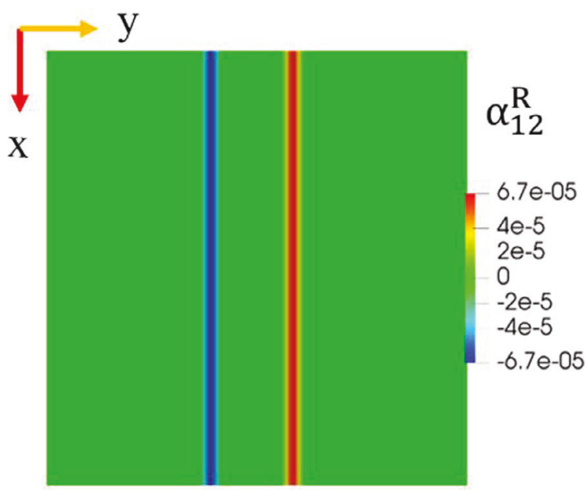

Fig. 7. The non-zero component of the referential dislocation density tensor plotted in the reference configuration. The dislocation lines pointing in the x (vertical) direction with referential Burgers vector in the y (horizontal) direction, pulled back from the microstructure configuration.

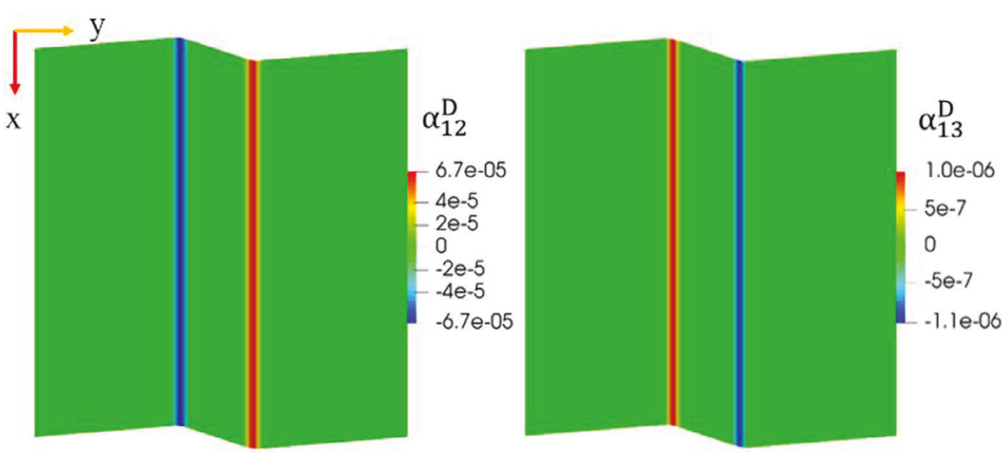

Fig. 8. Plot of the non-zero components of the deformed dislocation density tensor in the deformed configuration. The microstructure Burgers vector points in the y (horizontal) direction which gets pushed forward to the deformed configuration where it has non-zero y and z component. The α^{D}_{13} component (right) results from the rotation about the x-axis of the microstructure Burgers vector as it is pushed forward to the deformed configuration.

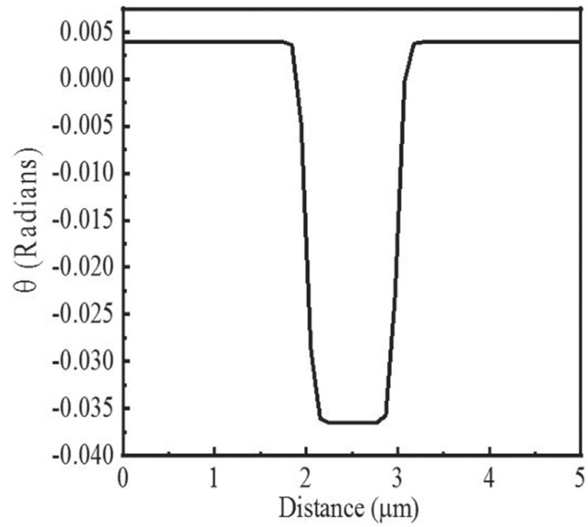

Fig. 9. A line profile of the angle of rotation of lattice planes about the x-axis caused by the elastic distortion induced by the two tilt boundaries. The line profile is along the y-direction.

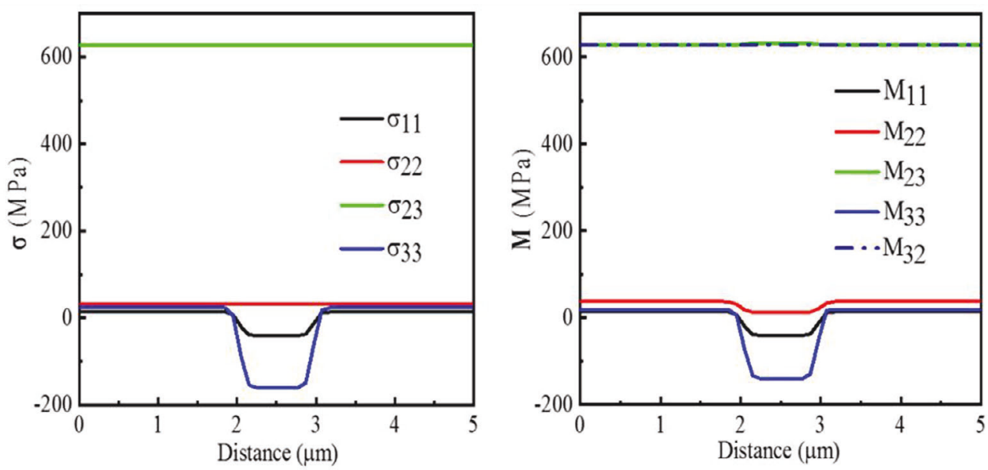

Fig. 10. Line profile plots of the Cauchy (left) and Mandel (right) stress components through the tilt boundaries in the reference configuration.

of most grains in deformed polycrystalline solids (Lin et al., 2010). In Liu et al. (1998) the angle across the tilt boundaries was on the order of 2 to 3°, matching the misorientation level measured at the plastic strain of 4% simulated here. The boundary separation was on the low side compared with the experimental observations at that strain level.

The ability to compute stress fields within and close to dislocation boundaries in deformed crystals will enable direct and absolute comparison with X-ray measurements of lattice stress at mesoscale of the type reported in Levine et al. (2011). The specific stress profile shown in Fig. 10 between the two tilt boundaries is due to the piecewise constant distribution of the resulting elastic strain. We note that this solution is also consistent with the 2D solution obtained in Brenner et al. (2014) for the symmetric tilt boundaries similar to the case presented here. In passing, we further remark that the symmetric tilt boundary simulated above is different from the single tilt boundary found in, say, Anderson et al. (2017), which shows a strongly decaying stress field.

8. Summary and conclusions

A continuum dislocation dynamics formulation suitable for investigating mesoscale crystal plasticity and dislocation patterning at finite deformation has been developed. In this formulation, the key equations consist of slip system level transport equations for vector densities of dislocations, coupled with finite deformation crystal mechanics. The coupling is two-way in the sense that crystal mechanics yields the driving force for dislocation motion while the motion of dislocation provides the plastic distortion required for stress update. The transport equations for both the spatial and referential vector densities of dislocations were derived in the spatial frame and referential frame, respectively. These equations are frame invariant, i.e., having the same form, with the one difference that the transport velocity is the velocity of dislocations relative to the lattice in the referential case, Eq. (76), versus the absolute velocity consisting of the same plus the crystal velocity in the spatial form (84) of the transport equations. The referential dislocation dynamics problem is summarized in Eq. (116), consisting of the stress equilibrium equation, dislocation transport equation, and a mobility law. The latter connects the dislocation velocity with a generalized Peach–Koehler force fixed in the reference configuration terms of Mandel stress, Eq. (113).

Several dislocation density tensors were defined, some of which were already used by other authors (Acharya, 2001; Cermelli and Gurtin, 2001). The two-point dislocation density tensors $\boldsymbol{\alpha}^{\mathrm{RM}}$ and $\boldsymbol{\alpha}^{\mathrm{DM}}$ were particularly useful in deriving the transport equations for the referential and spatial vector densities, respectively. Our derivation of all dislocation density and flux tensors relied on formulating the compatibility conditions in terms of an additive decomposition of the displacement and velocity gradients. The definitions of the resulting dislocation density tensors are consistent with those obtained from the multiplicative decomposition of the deformation gradient followed in the relevant literature. This makes our derivation similar to that used in the case of infinitesimal deformation, e.g., that by Kröner (1981), de Wit (1973b, 1973a) and others, while fully accounting for the kinematics of finite deformation. In Section 6, some aspects of the equivalence of the work reported in Gurtin (2006) were introduced at the level of transport equations for the tensor density fields, but differ in the results obtained for the transport of the vector densities.

Our development of the driving force for dislocations was based on thermodynamics. With a hypothesized free energy density that has both elastic and plastic (defect) contributions, Eq. (91), it was possible to reach the conventional hyperplastic stress-strain relationship for finite deformation, (106), and a generalized expression for the Peach–Koehler force, (113). The counterparts of such relationships for a dislocation tensor-based theory can be found in Acharya and Roy (2006). Two important observations are worth mentioning with regard to the generalized Peach-Koehler force expression obtained here. The first is that the elastic part of the Peach–Koehler force in the reference configuration is cast in terms of Mandel stress and the form is similar to that in the literature in terms of Cauchy stress, e.g., in Anderson et al. (2017). The second is that any additional energy associated with the presence of dislocations in the crystal and which evolves with the evolution of dislocations, will exert resistive force to dislocation motion via the term $\boldsymbol{\omega}^{(l)}$ in Eq. (113) for the driving force for the dislocation motion. This term, which depends on the gradient of the plastic (defect) part of the free energy with respect to the vector density of dislocation, offers the possibility to include, say, core energy of dislocation lines into the driving force for dislocation motion and couple dislocation motion with other types of defects in a more expanded theory.

The referential form of the dislocation transport equations was developed with a total Lagrange numerical treatment in mind. Initial development of that scheme was already carried out in solving the static test problems presented here, which were included to make a preliminary case of investigating the effects of lattice rotation in the context of finite deformation dislocation mechanics. The complete development, including a coupled solution of the continuum dislocation dynamics equations will be the subject of a more detailed future publication.

CRediT authorship contribution statement

Kyle Starkey: Conceptualization, Methodology, Software, Formal analysis, Investigation, Data curation, Writing - original draft, Visualization. **Grethe Winther:** Formal analysis, Investigation, Writing - review & editing. **Anter El-Azab:** Conceptualization, Methodology, Formal analysis, Investigation, Resources, Writing - original draft, Writing - review & editing, Supervision, Project administration, Funding acquisition.

Acknowledgment

This research was supported by the National Science Foundation, Division of Civil, Mechanical, and Manufacturing Innovation (CMMI) through award number 1663311 at Purdue University.

Supplementary materials

Supplementary material associated with this article can be found, in the online version, at doi:10.1016/j.jmps.2020.103926.

Appendix A. Transport equations for the dislocation density tensors

A.1. Rederiving Gurtin's transport equations for the microstructure dislocation density tensor

In this appendix, we show that the transport Eq. (70) for the two-point tensor $\boldsymbol{\alpha}^{\mathrm{DM}}$ is consistent with the derivation of the transport equations for the microstructure dislocation density tensor given in Gurtin (2006), which, in our notation, reads

$$\dot{\boldsymbol{\alpha}}^{\mathrm{M}} - \mathbf{L}^{\mathrm{p}}\boldsymbol{\alpha}^{\mathrm{M}} - \boldsymbol{\alpha}^{\mathrm{M}}\mathbf{L}^{\mathrm{pT}} = \mathbf{F}^{\mathbf{p}}\mathrm{Curl}_{\mathrm{L}^{\mathrm{p}}}(\mathbf{L}^{\mathrm{p}}\mathbf{F}^{\mathrm{p}}), \tag{A.1}$$

with $\mathrm{Curl}_{\mathbf{L}^p}(\mathbf{L}^p\mathbf{F}^p)$ being the Curl of $\mathbf{L}^p\mathbf{F}^p$ holding $\mathbf{F}^p$ fixed. We start by looking at the local transformation rule for $\boldsymbol{\alpha}^{\mathrm{M}}$ and the two-point tensor $\boldsymbol{\alpha}^{\mathrm{RM}}$, which is $\boldsymbol{\alpha}^{\mathrm{M}} = \frac{1}{\mathrm{J}^p}\mathbf{F}^p\boldsymbol{\alpha}^{\mathrm{RM}}$. Using relationship, we can then related the time derivatives of $\boldsymbol{\alpha}^{\mathrm{M}}$ and $\boldsymbol{\alpha}^{\mathrm{RM}}$ as follows:

$$\begin{aligned}\dot{\boldsymbol{\alpha}}^{\mathrm{M}} &= \left(\overline{\frac{1}{\mathrm{J}^p}\mathbf{F}^p}^{\boldsymbol{\cdot}}\right)\boldsymbol{\alpha}^{\mathrm{RM}} + \frac{1}{\mathrm{J}^p}\mathbf{F}^p\dot{\boldsymbol{\alpha}}^{\mathrm{RM}} \\ &= \left(\overline{\frac{1}{\mathrm{J}^p}}^{\boldsymbol{\cdot}}\mathbf{F}^p + \frac{1}{\mathrm{J}^p}\dot{\mathbf{F}}^p\right)\boldsymbol{\alpha}^{\mathrm{RM}} + \frac{1}{\mathrm{J}^p}\mathbf{F}^p\dot{\boldsymbol{\alpha}}^{\mathrm{RM}} = \left(-\frac{1}{\mathrm{J}^{p2}}\dot{\mathrm{J}}^p\mathbf{F}^p + \frac{1}{\mathrm{J}^p}\dot{\mathbf{F}}^p\right)\boldsymbol{\alpha}^{\mathrm{RM}} + \frac{1}{\mathrm{J}^p}\mathbf{F}^p\dot{\boldsymbol{\alpha}}^{\mathrm{RM}}.\end{aligned}$$

Using $\dot{\mathrm{J}}^p = \mathrm{J}^p\mathrm{tr}(\mathbf{L}^p)$, the above simplifies to: $\dot{\boldsymbol{\alpha}}^{\mathrm{M}} = -\mathbf{tr}(\mathbf{L}^p)\frac{1}{\mathrm{J}^p}\mathbf{F}^p\boldsymbol{\alpha}^{\mathrm{RM}} + \mathbf{L}^p\frac{1}{\mathrm{J}^p}\mathbf{F}^p\boldsymbol{\alpha}^{\mathrm{RM}} + \frac{1}{\mathrm{J}^p}\mathbf{F}^p\dot{\boldsymbol{\alpha}}^{\mathrm{RM}}$. Using the transformation relation between $\boldsymbol{\alpha}^{\mathrm{RM}}$ and $\boldsymbol{\alpha}^{\mathrm{M}}$, we can rewrite the first two terms on the right-hand side of the last expression to get,

$$\dot{\boldsymbol{\alpha}}^{\mathrm{M}} = -\mathbf{tr}(\mathbf{L}^p)\boldsymbol{\alpha}^{\mathrm{M}} + \mathbf{L}^p\boldsymbol{\alpha}^{\mathrm{M}} + \frac{1}{\mathrm{J}^p}\mathbf{F}^p\dot{\boldsymbol{\alpha}}^{\mathrm{RM}} \tag{A.2}$$

Or for glide only motion, $\mathrm{J}^p = 1$ and $\mathrm{tr}(\mathbf{L}^p) = 0$. Hence,

$$\dot{\boldsymbol{\alpha}}^{\mathrm{M}} - \mathbf{L}^p\boldsymbol{\alpha}^{\mathrm{M}} = \mathbf{F}^p\mathrm{Curl}(\phi)\ , \tag{A.3}$$

where we have used the compatibility condition (70) for $\boldsymbol{\alpha}^{\mathrm{RM}}$. Now, we can say that equation (A.3) ensures the compatibility of the total velocity field. We realize from (57), (23) and (18) that

$$\phi = \dot{\boldsymbol{\beta}}^p = \dot{\mathbf{F}}^p = \mathbf{L}^p\mathbf{F}^p, \tag{A.4}$$

and so we write (A.3) in the form,

$$\dot{\boldsymbol{\alpha}}^{\mathrm{M}} - \mathbf{L}^p\boldsymbol{\alpha}^{\mathrm{M}} = \mathbf{F}^p\mathrm{Curl}(\mathbf{L}^p\mathbf{F}^p).$$

Using the same notation to expand the product term in the Curl expression as used by Gurtin we get: $\dot{\boldsymbol{\alpha}}^{\mathrm{M}} - \mathbf{L}^p\boldsymbol{\alpha}^{\mathrm{M}} = \mathbf{F}^p(\mathrm{Curl}(\mathbf{F}^p)\mathbf{L}^{p\mathrm{T}} + \mathrm{Curl}_{\mathbf{L}^p}(\mathbf{L}^p\mathbf{F}^p))$. Using the definition of the microstructure dislocation density tensor (35) for glide only motion we can write,

$$\dot{\boldsymbol{\alpha}}^{\mathrm{M}} - \mathbf{L}^p\boldsymbol{\alpha}^{\mathrm{M}} - \boldsymbol{\alpha}^{\mathrm{M}}\mathbf{L}^{p\mathrm{T}} = \mathbf{F}^p\mathrm{Curl}_{\mathbf{L}^p}(\mathbf{L}^p\mathbf{F}^p),$$

which is (A.1) Gurtin, 2006). Starting with (72), a similar procedure will lead to this form of the transport equation for the microstructure dislocation density tensor.

A.2. Transport equations for the referential dislocation density tensor

In this appendix, we derive the transport relations for the referential dislocation density tensor, $\boldsymbol{\alpha}^{\mathrm{R}}$, starting from the transformation relations between $\boldsymbol{\alpha}^{\mathrm{RM}}$ and $\boldsymbol{\alpha}^{\mathrm{R}}$. This transformation has the form: $\boldsymbol{\alpha}^{\mathrm{RM}} = \boldsymbol{\alpha}^{\mathrm{R}}\mathbf{F}^{p\mathrm{T}}$, which by time differentiation yields: $\dot{\boldsymbol{\alpha}}^{\mathrm{RM}} = \dot{\boldsymbol{\alpha}}^{\mathrm{R}}\mathbf{F}^{p\mathrm{T}} + \boldsymbol{\alpha}^{\mathrm{R}}\dot{\mathbf{F}}^{p\mathrm{T}}$. By further using $\dot{\mathbf{F}}^p = \mathbf{L}^p\mathbf{F}^p$, $\dot{\mathbf{F}}^{p\mathrm{T}} = \mathbf{F}^{p\mathrm{T}}\mathbf{L}^{p\mathrm{T}}$, the last expression can be rewritten in the form: $\dot{\boldsymbol{\alpha}}^{\mathrm{RM}} = \dot{\boldsymbol{\alpha}}^{\mathrm{R}}\mathbf{F}^{p\mathrm{T}} + \boldsymbol{\alpha}^{\mathrm{R}}\mathbf{F}^{p\mathrm{T}}\mathbf{L}^{p\mathrm{T}} = \dot{\boldsymbol{\alpha}}^{\mathrm{R}}\mathbf{F}^{p\mathrm{T}} + \boldsymbol{\alpha}^{\mathrm{RM}}\mathbf{L}^{p\mathrm{T}}$, which finally leads to

$$\dot{\boldsymbol{\alpha}}^{\mathrm{RM}} - \boldsymbol{\alpha}^{\mathrm{RM}}\mathbf{L}^{p\mathrm{T}} = \dot{\boldsymbol{\alpha}}^{\mathrm{R}}\mathbf{F}^{p\mathrm{T}}.. \tag{A.5}$$

Using the compatibility condition (70) and expanding the flux term like in (A.4) gives,

$$\dot{\boldsymbol{\alpha}}^{\mathrm{RM}} = \mathrm{Curl}\left(\mathbf{L}^p\mathbf{F}^p\right) = \boldsymbol{\alpha}^{\mathrm{RM}}\mathbf{L}^{p\mathrm{T}} + \mathrm{Curl}_{\mathbf{L}^p}(\mathbf{L}^p\mathbf{F}^p). \tag{A.6}$$

Plugging (A.6) into (A.5) gives

$$\dot{\boldsymbol{\alpha}}^{\mathrm{R}} = \mathrm{Curl}_{\mathbf{L}^p}(\mathbf{L}^p\mathbf{F}^p)\mathbf{F}^{p-\mathrm{T}}, \tag{A.7}$$

which is the transport equations for the referential dislocation density tensor.

A.3. Transport equations for the spatial dislocation density tensor

In this appendix, we derive the transport relations for the spatial dislocation density tensor, $\boldsymbol{\alpha}^{\mathrm{D}}$. The starting point is the transformation relation between the dislocation density tensor in the deformed configuration and the two-point tensor $\boldsymbol{\alpha}^{\mathrm{DM}}$, which has the form: $\boldsymbol{\alpha}^{\mathrm{DM}} = \boldsymbol{\alpha}^{\mathrm{D}}\mathbf{F}^{e-\mathrm{T}}$. By further taking the material time derivative, we obtain $\dot{\boldsymbol{\alpha}}^{\mathrm{DM}} = \dot{\boldsymbol{\alpha}}^{\mathrm{D}}\mathbf{F}^{e-T} + \boldsymbol{\alpha}^{\mathrm{D}}\dot{\mathbf{F}}^{e-T} = \dot{\boldsymbol{\alpha}}^{\mathrm{D}}\mathbf{F}^{\mathbf{e}-\mathbf{T}} - \boldsymbol{\alpha}^{\mathrm{D}}\mathbf{L}^{\mathbf{eT}}\mathbf{F}^{\mathbf{e}-\mathbf{T}}$, which simplifies to:

$$\dot{\boldsymbol{\alpha}}^{\mathrm{D}} - \boldsymbol{\alpha}^{\mathrm{D}}\mathbf{L}^{\mathbf{eT}} = \dot{\boldsymbol{\alpha}}^{\mathrm{DM}}\mathbf{F}^{e\mathrm{T}}. \tag{A.8}$$

Inserting the compatibility condition (72) and solving for $\dot{\boldsymbol{\alpha}}^{\mathrm{D}}$ gives,

$$\dot{\boldsymbol{\alpha}}^{\mathrm{D}} + \mathrm{tr}(\mathbf{L})\boldsymbol{\alpha}^{\mathrm{D}} - \mathbf{L}\boldsymbol{\alpha}^{\mathrm{D}} - \boldsymbol{\alpha}^{\mathrm{D}}\mathbf{L}^{e\mathrm{T}} = \mathrm{curl}\left(\phi\mathbf{F}^{-1}\right)\ \mathbf{F}^{e\mathrm{T}}. \tag{A.9}$$

Expanding the dislocation current term,

$$\begin{aligned}\mathrm{curl}\left(\phi\mathbf{F}^{-1}\right)\mathbf{F}^{\mathrm{eT}} &= \mathrm{curl}\left(\mathbf{L}^{\mathrm{p}}\mathbf{F}^{\mathrm{e}-1}\right)\mathbf{F}^{\mathrm{eT}} \\ &= \mathrm{curl}\left(\mathbf{F}^{\mathrm{e}-1}\right)\mathbf{L}^{\mathrm{pT}}\mathbf{F}^{\mathrm{eT}} + \mathrm{curl}_{\mathrm{L^p}}\left(\mathbf{L}^{\mathrm{p}}\mathbf{F}^{\mathrm{e}-1}\right)\mathbf{F}^{\mathrm{eT}}.\end{aligned}$$

We can also write,

$$\begin{aligned}\mathrm{curl}\left(\mathbf{F}^{\mathrm{e}-1}\right)\mathbf{L}^{\mathrm{pT}}\mathbf{F}^{\mathrm{eT}} &= \mathrm{curl}\left(\mathbf{F}^{\mathrm{e}-1}\right)\mathbf{F}^{\mathrm{eT}}\mathbf{F}^{\mathrm{e}-\mathrm{T}}\mathbf{L}^{\mathrm{pT}}\mathbf{F}^{\mathrm{eT}} \\ &= \boldsymbol{\alpha}^{\mathrm{D}}\mathbf{F}^{\mathrm{e}-\mathrm{T}}\mathbf{L}^{\mathrm{pT}}\mathbf{F}^{\mathrm{eT}} = \boldsymbol{\alpha}^{\mathrm{D}}\left(\mathbf{L}^{\mathrm{T}} - \mathbf{L}^{\mathrm{eT}}\right),\end{aligned}$$

which leads to,

$$\mathrm{curl}\left(\phi\mathbf{F}^{-1}\right)\mathbf{F}^{\mathrm{eT}} = \boldsymbol{\alpha}^{\mathrm{D}}\left(\mathbf{L}^{\mathrm{T}} - \mathbf{L}^{\mathrm{eT}}\right) + \mathrm{curl}_{\mathrm{L^p}}\left(\mathbf{L}^{\mathrm{p}}\mathbf{F}^{e-1}\right)\mathbf{F}^{\mathrm{eT}}. \tag{A.10}$$

Substituting this expansion into (A.9) and rearranging terms gives the transport equations for the dislocation density tensor in the deformed configuration,

$$\dot{\boldsymbol{\alpha}}^{\mathrm{D}} + \mathrm{tr}(\mathbf{L})\boldsymbol{\alpha}^{\mathrm{D}} - \mathbf{L}\boldsymbol{\alpha}^{\mathrm{D}} - \boldsymbol{\alpha}^{\mathrm{D}}\mathbf{L}^{\mathrm{T}} = \mathrm{curl}_{\mathrm{L^p}}\left(\mathbf{L}^{\mathrm{p}}\mathbf{F}^{e-1}\right)\mathbf{F}^{\mathrm{eT}}. \tag{A.11}$$

In this equation, the left-hand side is Oldroyd derivative Oldroyd, 1950). The same expression can be derived by looking at the transformation relationship between the referential dislocation density tensor and the deformed tensor by taking its material time derivative and plugging in (A.7) for the $\dot{\boldsymbol{\alpha}}^{\mathrm{R}}$. Using the relationships between the dislocation currents in ((54) we obtain a relationship for the curl terms as: $\mathrm{Curl}_{\mathrm{L^p}}(\mathbf{L}^{\mathrm{p}}\mathbf{F}^{\mathrm{p}}) = J\mathbf{F}^{-1}\mathrm{curl}_{\mathrm{L^p}}(\mathbf{L}^{\mathrm{p}}\mathbf{F}^{e-1})$, which is needed to show that (A.11) is consistent with (A.7).

Appendix B. Simplifying power of deformation in reference configuration

In this appendix, we explain the details of reaching Eq. (89) starting from (88). Expanding the first material time derivative term and further using $\dot{\mathbf{F}}^{\mathrm{p}} = \phi$, we reach $(\overline{\mathbf{F}^{\mathrm{pT}}\mathbf{E}^{\mathrm{e}}\mathbf{F}^{\mathrm{p}}})^{\cdot} = \phi^{\mathrm{T}}\mathbf{E}^{\mathrm{e}}\mathbf{F}^{\mathrm{p}} + \mathbf{F}^{\mathrm{pT}}\mathbf{E}^{\mathrm{e}}\phi + \mathbf{F}^{\mathrm{pT}}\dot{\mathbf{E}}^{\mathrm{e}}\mathbf{F}^{\mathrm{p}}$. The first two terms in the last expression are both related to the motion of dislocations. They are segregated in the form:

$$\mathbf{Q}^{\mathrm{p}} \equiv \phi^{\mathbf{T}}\mathbf{E}^{\mathrm{e}}\mathbf{F}^{\mathrm{p}} + \mathbf{F}^{\mathrm{pT}}\mathbf{E}^{\mathrm{e}}\phi. \tag{B.1}$$

The last term is related to the rate of elastic strain. Looking at the second term, $\mathbf{S} : \dot{\mathbf{E}}^{\mathbf{p}}$ in Eq. (88) and expanding $\dot{\mathbf{E}}^{\mathbf{p}}$ we get: $\dot{\mathbf{E}}^{\mathrm{p}} = \dot{\mathbf{C}}^{\mathrm{p}} = 1/2(\dot{\mathbf{F}}^{\mathrm{pT}}\mathbf{F}^{\mathrm{p}} + \mathbf{F}^{\mathrm{pT}}\dot{\mathbf{F}}^{\mathrm{p}}) = 1/2(\mathbf{F}^{\mathrm{pT}}\mathbf{L}^{\mathrm{p}}\mathbf{F}^{\mathrm{p}} + \mathbf{F}^{\mathrm{pT}}\mathbf{L}^{\mathrm{p}}\mathbf{F}^{\mathrm{p}})$. Since this term will be contracted with a symmetric tensor we can write: $\mathbf{S} : \dot{\mathbf{E}}^{\mathrm{p}} = \mathbf{S} :\ 1/2(\mathbf{F}^{\mathrm{pT}}\mathbf{L}^{\mathrm{p}}\mathbf{F}^{\mathrm{p}} + \mathbf{F}^{\mathrm{pT}}\mathbf{L}^{\mathrm{p}}\mathbf{F}^{\mathrm{p}}) = \mathbf{S} : (\mathbf{F}^{\mathrm{pT}}\mathbf{L}^{\mathrm{p}}\mathbf{F}^{\mathrm{p}})$. We also notice that, since $\dot{\mathbf{F}}^{\mathrm{p}} = \mathbf{L}^{\mathrm{p}}\mathbf{F}^{\mathrm{p}}$, we can replace the last term with $\mathbf{S} : (\mathbf{F}^{\mathrm{pT}}\dot{\mathbf{F}}^{\mathrm{p}})$, and by the definition of $\boldsymbol{\beta}^{\mathrm{p}}$, we have $\dot{\mathbf{F}}^{\mathrm{p}} = \dot{\boldsymbol{\beta}}^{\mathrm{p}} = \phi$. Then $\mathbf{S} : \dot{\mathbf{E}}^{\mathrm{p}} =\ \mathbf{S} : (\mathbf{F}^{\mathrm{pT}}\phi) = \mathbf{S} : (\mathbf{F}^{\mathrm{pT}}\mathbf{F}^{\mathrm{p}}\mathbf{F}^{\mathrm{p}-1}\phi) = \mathbf{S} : (\mathbf{C}^{\mathrm{p}}\mathbf{F}^{\mathrm{p}-1}\phi)$. Using properties of the double inner product we reach

$$\mathbf{S} : \dot{\mathbf{E}}^{\mathrm{p}} = \left(\mathbf{C}^{\mathrm{pT}}\mathbf{S}\right) : \left(\mathbf{F}^{\mathrm{p}-1}\phi\right) = (\mathbf{C}^{\mathrm{p}}\mathbf{S}) : \left(\mathbf{F}^{\mathrm{p}-1}\phi\right). \tag{B.2}$$

Now we will work on the $\mathbf{Q}^{\mathrm{p}}$ term.

$$\mathbf{S} : \mathbf{Q}^{\mathrm{p}} = \mathbf{S} : \left(\phi^{\mathrm{T}}\mathbf{E}^{\mathrm{e}}\mathbf{F}^{\mathrm{p}}\right) + \mathbf{S} : \left(\mathbf{F}^{\mathrm{pT}}\mathbf{E}^{\mathrm{e}}\phi\right). \tag{B.3}$$

For the first term we use the double inner product property (13), $\mathbf{A} : \mathbf{B} = \mathbf{A}^{\mathrm{T}} : \mathbf{B}^{\mathrm{T}}$, which yields: $\mathbf{S} : (\phi^{\mathrm{T}}\mathbf{E}^{\mathrm{e}}\mathbf{F}^{\mathrm{p}}) = \mathbf{S}^{\mathrm{T}} : [(\mathbf{E}^{\mathrm{e}}\mathbf{F}^{\mathrm{p}})^{\mathrm{T}}\phi] = \mathbf{S} : [(\mathbf{E}^{\mathrm{e}}\mathbf{F}^{\mathrm{p}})^{\mathrm{T}}\phi]$. Then using (14) leads to $\mathbf{S} : (\phi^{\mathrm{T}}\mathbf{E}^{\mathrm{e}}\mathbf{F}^{\mathrm{p}}) = [\mathbf{E}^{\mathrm{e}}\mathbf{F}^{\mathrm{p}}\mathbf{S}] : \phi$. Applying the same inner product property (14) to the second term in (B.3) gives $\mathbf{S} : (\mathbf{F}^{\mathrm{pT}}\mathbf{E}^{\mathrm{e}}\phi) = [\mathbf{E}^{\mathrm{eT}}\mathbf{F}^{\mathrm{p}}\mathbf{S}] : \phi = [\mathbf{E}^{\mathrm{e}}\mathbf{F}^{\mathrm{p}}\mathbf{S}] : \phi$, and so we reach

$$\mathbf{S} : \mathbf{Q}^{\mathrm{p}} = 2[\mathbf{E}^{\mathrm{e}}\mathbf{F}^{\mathrm{p}}\mathbf{S}] : \phi. \tag{B.4}$$

We choose to write (B.4) in the form: $2[\mathbf{E}^{\mathrm{e}}\mathbf{F}^{\mathrm{p}}\mathbf{S}] : \phi = 2[\mathbf{E}^{\mathrm{e}}\mathbf{F}^{\mathrm{p}}\mathbf{S}] : \mathbf{F}^{\mathrm{p}}(\mathbf{F}^{p-1}\phi) = 2[\mathbf{F}^{\mathrm{pT}}\mathbf{E}^{\mathrm{e}}\mathbf{F}^{\mathrm{p}}\mathbf{S}] : (\mathbf{F}^{p-1}\phi) = 2[\mathbf{E}^{\mathrm{e}}_{\mathrm{R}}\mathbf{S}] : (\mathbf{F}^{p-1}\phi)$, so that the power of deformation in the reference configuration becomes: $\mathbf{S} : \dot{\mathbf{E}} = \{(2\mathbf{E}^{\mathrm{e}}_{\mathrm{R}} + \mathbf{C}^{\mathrm{p}})\mathbf{S}\} : (\mathbf{F}^{\mathrm{p}-1}\phi) + \mathbf{S} : (\mathbf{F}^{\mathrm{pT}}\dot{\mathbf{E}}^{\mathrm{e}}\mathbf{F}^{\mathrm{p}})$. We further simplify the first term as follows,

$$\begin{aligned}\left(2\mathbf{E}^{\mathrm{e}}_{\mathrm{R}} + \mathbf{C}^{\mathrm{p}}\right)\mathbf{S} &= 2(\mathbf{E} - \mathbf{E}^{\mathrm{p}})\mathbf{S} + \mathbf{C}^{\mathrm{p}}\mathbf{S} \\ &= 2\mathbf{ES} - 2\left(\tfrac{1}{2}[\mathbf{C}^{\mathrm{p}} - \mathbf{I}]\right)\mathbf{S} + \mathbf{C}^{\mathrm{p}}\mathbf{S} \\ &= 2\mathbf{ES} + \mathbf{S} = (2\mathbf{E} + \mathbf{I})\mathbf{S} = \mathbf{CS} = \mathbf{M},\end{aligned}$$

with $\mathbf{M} = \mathbf{CS}$ being the referential Mandel stress. This completes the rewriting of Eq. (88) into (89).

Appendix C. Constitutive analysis in the deformed configuration

The statement of global free energy imbalance expressed in the deformed configuration, ignoring entropic effects, reads

$$\int \left(\rho_D\dot{\psi}_D - \boldsymbol{\sigma} : \mathbf{L}\right)\mathrm{dv_D} \leq 0, \tag{C.1}$$

where ψ_D is the specific free energy in the deformed configuration and ρ_D is the mass density. We use the fact that $\dot{\mathbf{F}}^{\mathrm{p}} = \dot{\boldsymbol{\beta}}^{\mathrm{p}} = \boldsymbol{\phi}$, (16), (18) and (62) to write the velocity gradient as $\mathbf{L} = \mathbf{L}^{\mathbf{e}} + \mathbf{F}^{\mathbf{e}} \sum_l \mathbf{b}_{\mathrm{M}}^{(l)} \otimes (\mathbf{v}_{\mathrm{D}}^{(l)} \times \boldsymbol{\rho}_{\mathrm{D}}^{(l)})$. From, $\mathbf{F}^{\mathbf{e}}\mathbf{b}_{\mathrm{M}}^{(l)} = \mathbf{b}_{\mathrm{D}}^{(l)}$, and (17)

$$\mathbf{L} = \dot{\mathbf{F}}^{\mathrm{e}}\mathbf{F}^{\mathrm{e}-1} + \sum_l \mathbf{b}_{\mathrm{D}}^{(l)} \otimes \left(\mathbf{v}_{\mathrm{D}}^{(l)} \times \boldsymbol{\rho}_{\mathrm{D}}^{(l)}\right). \tag{C.2}$$

Then using (14), the free energy imbalance becomes,

$$\int \left(\rho_D \dot{\psi}_D - \left(\boldsymbol{\sigma}\mathbf{F}^{\mathrm{e}-\mathrm{T}}\right) : \dot{\mathbf{F}}^{\mathrm{e}} - \boldsymbol{\sigma} : \left(\sum_l \mathbf{b}_{\mathrm{D}}^{(l)} \otimes \left(\mathbf{v}_{\mathrm{D}}^{(l)} \times \boldsymbol{\rho}_{\mathrm{D}}^{(l)}\right)\right)\right) \mathrm{d}v_{\mathrm{D}} \leq 0. \tag{C.3}$$

Let us rewrite the specific free energy in the form:

$$\psi_{\mathrm{D}} = \hat{\psi}_{\mathrm{D}}^{\mathrm{e}}(\mathbf{F}^{\mathrm{e}}) + \hat{\psi}_{\mathrm{D}}^{\mathrm{p}}\left(\boldsymbol{\rho}_{\mathrm{R}}^{(l)}\right). \tag{C.4}$$

Taking the material time derivative of the elastic term gives: $\dot{\psi}_{\mathrm{D}}^{\mathrm{e}} = \frac{\partial \hat{\psi}_{\mathrm{D}}^{\mathrm{e}}}{\partial \mathbf{F}^{\mathbf{e}}} : \dot{\mathbf{F}}^{\mathbf{e}}$. Plugging this into the free energy imbalance yields,

$$\int \left(\left(\rho_D \frac{\partial \hat{\psi}_{\mathrm{D}}^{\mathrm{e}}}{\partial \mathbf{F}^{\mathbf{e}}} - \boldsymbol{\sigma}\mathbf{F}^{\mathrm{e}-\mathrm{T}}\right) : \dot{\mathbf{F}}^{\mathrm{e}} + \rho_D \dot{\psi}_{\mathrm{D}}^{\mathrm{p}} - \boldsymbol{\sigma} : \left(\sum_l \mathbf{b}_{\mathrm{D}}^{(l)} \otimes \left(\mathbf{v}_{\mathrm{D}}^{(l)} \times \boldsymbol{\rho}_{\mathrm{D}}^{(l)}\right)\right)\right) \mathrm{d}v_{\mathrm{D}} \leq 0. \tag{C.5}$$

Using the transformation relation between the Cauchy stress and the PK1 stress in the microstructure configuration, $\boldsymbol{\sigma}\mathbf{F}^{e-T} = J^{e-1}\mathbf{P}^{\mathbf{e}}$, and the fact that there is no dissipation for the elastic terms we arrive at $\mathbf{P}^{\mathrm{e}} \equiv \rho_{\mathrm{M}} \frac{\partial \hat{\psi}_{\mathrm{D}}^{\mathrm{e}}}{\partial \mathbf{F}^{\mathbf{e}}}$ just like in (105). We now focus on the plastic terms.

We start by noticing a relationship between the material time derivative and the Oldroyd derivative. From $\boldsymbol{\rho}_{\mathrm{R}} = J\mathbf{F}^{-1}\boldsymbol{\rho}_{\mathrm{D}}$, and taking the material time derivative of both sides (42) we can write,

$$\dot{\boldsymbol{\rho}}_{\mathrm{R}} = \mathrm{J}\mathbf{F}^{-1}\left(\dot{\boldsymbol{\rho}}_{\mathrm{D}} + (\mathrm{tr}(\mathbf{L})\mathbf{I} - \mathbf{L})\boldsymbol{\rho}_{\mathrm{D}}\right). \tag{C.6}$$

We note that the term following $\mathrm{J}\mathbf{F}^{-1}$ in the above expression is the Oldroyd derivative of the spatial vector density, which is a frame indifferent time derivative. Recalling in (C.4) that we have the constitutive form: $\psi_{\mathrm{D}}^{\mathrm{p}} = \hat{\psi}_{\mathrm{D}}^{\mathrm{p}}(\boldsymbol{\rho}_{\mathrm{R}}^{(l)})$, which is a frame indifferent constitutive function due to its dependence on the referential dislocation density. We now show that this is equivalent a form in which $\hat{\psi}_{\mathrm{D}}^{\mathrm{p}}$ depends on the spatial dislocation density, $\boldsymbol{\rho}_{\mathrm{D}}^{(l)}$. Taking the material time derivative of $\psi_{\mathrm{D}}^{\mathrm{p}} = \hat{\psi}_{\mathrm{D}}^{\mathrm{p}}(\boldsymbol{\rho}_{\mathrm{R}}^{(l)})$, and using (C.6) gives,

$$\begin{aligned}\dot{\psi}_{\mathrm{D}}^{\mathrm{p}} &= \sum_l \frac{\partial \hat{\psi}_{\mathrm{D}}^{\mathrm{p}}}{\partial \boldsymbol{\rho}_{R}^{(l)}} \cdot \dot{\boldsymbol{\rho}}_{\mathrm{R}}^{(l)} \\ &= \sum_l \frac{\partial \hat{\psi}_{\mathrm{D}}^{\mathrm{p}}}{\partial \boldsymbol{\rho}_{R}^{(l)}} \cdot \left[\mathrm{J}\mathbf{F}^{-1}\left(\dot{\boldsymbol{\rho}}_{\mathrm{D}}^{(l)} + (\mathrm{tr}(\mathbf{L})\mathbf{I} - \mathbf{L})\boldsymbol{\rho}_{\mathrm{D}}^{(l)}\right)\right].\end{aligned} \tag{C.7}$$

From $\boldsymbol{\rho}_{\mathrm{R}}^{(l)} = J\mathbf{F}^{-1}\boldsymbol{\rho}_{\mathrm{D}}^{(l)}$, we have that, $\frac{\partial \boldsymbol{\rho}_{R}^{(l)}}{\partial \boldsymbol{\rho}_{\mathrm{D}}^{(l)}} = J\mathbf{F}^{-1}$. Plugging this into the last expression gives,

$$\begin{aligned}\dot{\psi}_{\mathrm{D}}^{\mathrm{p}} &= \sum_l \frac{\partial \hat{\psi}_{\mathrm{D}}^{\mathrm{p}}}{\partial \boldsymbol{\rho}_{R}^{(l)}} \frac{\partial \boldsymbol{\rho}_{R}^{(l)}}{\partial \boldsymbol{\rho}_{\mathrm{D}}^{(l)}} \left(\dot{\boldsymbol{\rho}}_{\mathrm{D}}^{(l)} + (\mathrm{tr}(\mathbf{L})\mathbf{I} - \mathbf{L})\boldsymbol{\rho}_{\mathrm{D}}^{(l)}\right) \\ &= \sum_l \frac{\partial \hat{\psi}_{\mathrm{D}}^{\mathrm{p}}}{\partial \boldsymbol{\rho}_{\mathrm{D}}^{(l)}} \left(\dot{\boldsymbol{\rho}}_{\mathrm{D}}^{(l)} + (\mathrm{tr}(\mathbf{L})\mathbf{I} - \mathbf{L})\boldsymbol{\rho}_{\mathrm{D}}^{(l)}\right)\end{aligned} \tag{C.8}$$

By using the transport relationship (80) without the network term into the last equation, we reach

$$\dot{\psi}_{\mathrm{D}}^{\mathrm{p}} = \sum_l \frac{\partial \hat{\psi}_{\mathrm{D}}^{\mathrm{p}}}{\partial \boldsymbol{\rho}_{\mathrm{D}}^{(l)}} \mathrm{curl}\left(\mathbf{v}_{\mathrm{D}}^{(l)} \times \boldsymbol{\rho}_{\mathrm{D}}^{(l)}\right). \tag{C.9}$$

Both (C.8) and (C.9) suggest that the constitutive function $\hat{\psi}_{\mathrm{D}}^{\mathrm{p}}$ should depend on the spatial dislocation density, $\boldsymbol{\rho}_{\mathrm{D}}^{(l)}$. That is, $\psi_{\mathrm{D}}^{\mathrm{p}} = \hat{\psi}_{\mathrm{D}}^{\mathrm{p}}(\boldsymbol{\rho}_{\mathrm{D}}^{(l)})$. General treatments leading to frame indifference of the spatial constitutive laws in dissipative systems have also been explored in Morro (2010) and Ván (2008). Multiplying both sides of (C.9) by the mass density ρ_{D}

$$\rho_{\mathrm{D}} \dot{\psi}_{\mathrm{D}}^{\mathrm{p}} = \sum_l \frac{\partial\left(\rho_{\mathrm{D}} \hat{\psi}_{\mathrm{D}}^{\mathrm{p}}\right)}{\partial \boldsymbol{\rho}_{\mathrm{D}}^{(l)}} \mathrm{curl}\left(\mathbf{v}_{\mathrm{D}}^{(l)} \times \boldsymbol{\rho}_{\mathrm{D}}^{(l)}\right), \tag{C.10}$$

and borrowing arguments from the text that lead to (111), namely, the equation before (107) and those leading up to (111), we may write,

$$\int^{\rho_D} \dot{\psi}^{\mathrm{p}}_{\mathrm{D}} d v_{\mathrm{D}} = -\int \sum_{l} \rho^{(l)}_{\mathrm{D}} \mathbf{v}^{(l)}_{\mathrm{D}} \cdot \left[\mathrm{curl}\left(\frac{\partial \widehat{\psi}^{\mathrm{p}}_{\mathrm{D}}}{\partial \boldsymbol{\rho}^{(l)}_{\mathrm{D}}} \right) \times \boldsymbol{\xi}^{(l)}_{\mathrm{D}} \right] \mathrm{d} v_{\mathrm{D}}. \tag{C.11}$$

with $\widehat{\psi}^{\mathrm{p}}_{\mathrm{D}} = \rho_{\mathrm{D}} \hat{\psi}^{\mathrm{p}}_{\mathrm{D}}$. With these simplification, the plastic free energy imbalance terms in (C.5) becomes

$$\int -\sum_{l} \rho^{(l)}_{\mathrm{D}} \mathbf{v}^{(l)}_{\mathrm{D}} \cdot \left[\left(\mathbf{b}^{(l)}_{\mathrm{D}} \cdot \boldsymbol{\sigma}^{\mathrm{T}} + \boldsymbol{\omega}^{(l)}_{\mathrm{D}} \right) \times \boldsymbol{\xi}^{(l)}_{\mathrm{D}} \right] \mathrm{d}v_{\mathrm{D}} \leq 0. \tag{C.12}$$

In the above, we have employed a simplification similar to the one used in (107) to factor out the dislocation velocity term and used $\boldsymbol{\omega}^{(l)}_{\mathrm{D}} \equiv \mathrm{curl}(\frac{\partial \widehat{\psi}^{\mathrm{p}}_{\mathrm{D}}}{\partial \boldsymbol{\rho}^{(l)}_{\mathrm{D}}})$. We may thus define the spatial Peach-Koehler force at finite deformation by,

$$\mathbf{f}^{(l)}_{\mathrm{D}} = \left(\mathbf{b}^{(l)}_{\mathrm{D}} \cdot \boldsymbol{\sigma}^{\mathrm{T}} + \boldsymbol{\omega}^{(l)}_{\mathrm{D}} \right) \times \boldsymbol{\xi}^{(l)}_{\mathrm{D}}, \tag{C.13}$$

which takes a form similar to the referential driving force in (113). We could then use the Peach-Koehler force above into a mobility law, say: $\mathbf{v}^{(l)}_{\mathrm{D}} = M\mathbf{f}^{(l)}_{\mathrm{D}}$, to show that the dissipation term always remains positive.

In passing, we note that a form comparable to (C.13) was derived in Acharya and Roy (2006) for a tensor representation of the dislocation density. In that form, a properly defined Cauchy stress appears in an expression for the dissipation in a quantity serving as the work conjugate for a velocity quantity defined on the basis of a density tensor representation of dislocations. That form reduces to the part $(\mathbf{b}^{(l)}_{\mathrm{D}} \cdot \boldsymbol{\sigma}^{\mathrm{T}}) \times \boldsymbol{\xi}^{(l)}_{\mathrm{D}}$ in (C.13) in the case of single slip system and the bundle representation of dislocations we adopt in our work, where the velocity in our case is definable and represents the local dislocation velocity. See also Acharya (2011) for a related treatment of thermodynamics with a significantly different representation of the dislocation system in the constitutive hypothesis.

Appendix D. Arbitrary reference configuration

In order to show what constraints are implied in the choice of reference configuration we set up a set of mappings as depicted in Fig. D1. In addition to the three usual configurations, the reference **B**, microstructure, **M**, and spatial, **D**, we introduce a second arbitrary reference configuration, **B'**, that is generated from **B** via an arbitrary map **G**. We keep in mind here that the spatial (deformed) configuration **D** is the physical configuration of the material in its current state that is expressed in terms of the elastic and the defect states of the material. This deformed configuration **D** is obtained by mapping from the microstructure configuration **M** via the elastic distortion, $\mathbf{F}^{\mathrm{e}}$, which is uniquely connected to the defect state. As such, in investigating the dependence of the theoretical development presented here on the reference configuration, we must maintain the uniqueness of the deformed state and its connection with the microstructure configurations as they, together, represent the physical state of the material.

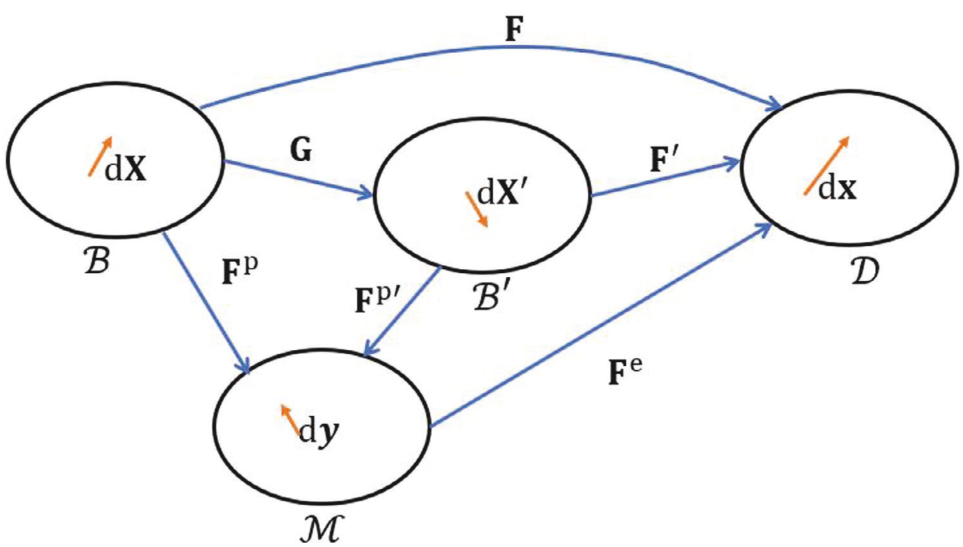

Fig. D1. Depiction of the mapping relations showing two reference configurations denoted by their respective differential line elements d**X** and d**X**′ related to each other by an arbitrary tangent map **G.** Note that the addition of the primed reference configuration means that there are now two routes to the deformed configuration through the microstructure configuration.

Given the above argument, we then think of multiple reference configurations being mapped to the same microstructure configuration via different plastic distortions. Thus, two plastic distortions $\mathbf{F}^{\boldsymbol{p}}$ and $\mathbf{F}^{\boldsymbol{p}'}$ are to be used to reach the microstructure configuration **M** from the two reference configurations **B** and **B'**. The corresponding (total) deformation gradients mapping these reference configurations to the deformed configuration are $\mathbf{F} = \mathbf{F}^{\mathrm{e}}\mathbf{F}^{\boldsymbol{p}}$ and $\mathbf{F}' = \mathbf{F}^{\mathrm{e}}\mathbf{F}^{\boldsymbol{p}'}$. From this we get the relations previously derived in the paper, namely (22) and (23) in addition to another set of relations,

$$\mathrm{d}\mathbf{u}' = \boldsymbol{\beta}'\mathrm{d}\mathbf{X} = \boldsymbol{\beta}^{\mathrm{p}'}\mathrm{d}\mathbf{X}' + \boldsymbol{\beta}^{\mathrm{e}}\mathrm{d}\mathbf{x} \tag{D.1}$$

where,

$$\boldsymbol{\beta}^{\mathrm{p}'} \equiv \mathbf{F}^{\mathrm{p}'} - \mathbf{I} \tag{D.2}$$

and $\boldsymbol{\beta}^{\mathrm{e}}$ is still defined by (23). Locally we also have that $\mathrm{d}\mathbf{X}' = \mathbf{G}\mathrm{d}\mathbf{X}$, for some arbitrary prescribed tangent map **G**. In order to study the arbitrariness of the reference configuration we study the map **G** to see if any restrictions are placed on it. Implicit in our formulation are the assumption of the compactness of the reference and deformed configuration, which gave rise to the compatibility of the displacement, $\oint \mathrm{d}\mathbf{u} = \oint \boldsymbol{\beta}^{\mathrm{p}}\mathrm{d}\mathbf{X} + \oint \boldsymbol{\beta}^{\mathrm{e}}\mathrm{d}\mathbf{x} = 0$, for the displacement field that maps the reference configuration **B** onto the spatial, **D**. Similarly, we have $\oint \mathrm{d}\mathbf{u}' = 0$ for the displacement field mapping the second reference configuration **B'** onto the spatial **D**. Expanding this expression gives $\oint \mathrm{d}\mathbf{u} = \oint \boldsymbol{\beta}^{\mathrm{p}'}\mathrm{d}\mathbf{X}' + \oint \boldsymbol{\beta}^{\mathrm{e}}\mathrm{d}\mathbf{x}$. Since the deformation paths share the same microstructure space, $\oint \boldsymbol{\beta}^{\mathrm{e}}\mathrm{d}\mathbf{x}$ is common to both compatibility constraints, from which we conclude that the reference configurations must be related by,

$$\oint \boldsymbol{\beta}^{\mathrm{p}}\mathrm{d}\mathbf{X} = -\oint \boldsymbol{\beta}^{\mathrm{e}}\mathrm{d}\mathbf{x} = \oint \boldsymbol{\beta}^{\mathrm{p}'}\mathrm{d}\mathbf{X}'. \tag{D.3}$$

Using the local relation, $\mathrm{d}\mathbf{X}' = \mathbf{G}\mathrm{d}\mathbf{X}$ and $\mathbf{F}^{\mathrm{p}'} = \mathbf{F}^{\mathrm{p}}\mathbf{G}^{-1}$ (from the diagram above), using (D.3) we can get a restriction on **G**,

$$\begin{aligned}\oint \boldsymbol{\beta}^{\mathrm{p}}\mathrm{d}\mathbf{X} &= \oint \left(\mathbf{F}^{\mathrm{p}'} - \mathbf{I}\right)\mathbf{G}\mathrm{d}\mathbf{X} \\ &= \oint \left(\mathbf{F}^{\mathrm{p}}\mathbf{G}^{-1} - \mathbf{I}\right)\mathbf{G}\mathrm{d}\mathbf{X} = \oint \mathbf{F}^{\mathrm{p}} - \mathbf{G}\mathrm{d}\mathbf{X} \\ &= \oint (\mathbf{F}^{\mathrm{p}} - \mathbf{I})\mathrm{d}\mathbf{X} + \oint (\mathbf{I} - \mathbf{G})\mathrm{d}\mathbf{X} \\ &= \oint \boldsymbol{\beta}^{\mathrm{p}}\mathrm{d}\mathbf{X} + \oint (\mathbf{I} - \mathbf{G})\mathrm{d}\mathbf{X}\end{aligned} \tag{D.4}$$

From (D.4) we see that the term $\oint(\mathbf{I} - \mathbf{G})\mathrm{d}\mathbf{X}$ should vanish. This means that **G** must be the derivative of some map, which means that the reference configuration is arbitrary up to compatible deformations. This result is very intuitive when considering topological defects, in that compatible maps should not change the nature of these defects, thus leaving (31) unchanged. Since the reference configuration is arbitrary up to compatible maps we can think of this map, **G**, as just a relabeling of material points. An example of this is when we take the reference configuration to be the deformed configuration, by setting $\mathbf{G} \to \mathbf{F}'^{-1}$ we get, $\mathbf{F} \to \mathbf{I}$ and thus $\mathbf{F}^{\mathrm{p}} = \mathbf{F}^{e-1}$. The Mandel stress then becomes equivalent to the Cauchy stress and the form invariance of equations (D.1) with (113) and (84) with (76) become identical, where we would have to make use of the fact that, in this case, the material and spatial time derivatives coincide.

For computational purposes, however, we have taken the reference configuration to be the defect-free configuration. Such a choice is natural because the defects themselves are defined relative to the defect free state. In this case, the possible class of the tangent maps **G** may include the class of compatible elastic deformations because such deformation do not alter the defect state of the material.

References

Acharya, A., 2011. Microcanonical entropy and mesoscale dislocation mechanics and plasticity. J. Elast. 104, 23–44. doi:10.1007/s10659-011-9328-3.

Acharya, A., 2004. Constitutive analysis of finite deformation field dislocation mechanics. J. Mech. Phys. Solids 52, 301–316. doi:10.1016/S0022-5096(03)00093-0.

Acharya, A., 2001. A model of crystal plasticity based on the theory of continuously distributed dislocations. J. Mech. Phys. Solids 49, 761–784. doi:10.1016/S0022-5096(00)00060-0.

Acharya, A., Roy, A., 2006. Size effects and idealized dislocation microstructure at small scales: predictions of a phenomenological model of mesoscopic field dislocation mechanics: part I. J. Mech. Phys. Solids 54, 1687–1710. doi:10.1016/j.jmps.2006.01.009.

Acharya, A., Roy, A., Sawant, A., 2006. Continuum theory and methods for coarse-grained, mesoscopic plasticity. Scr. Mater. 54, 705–710. doi:10.1016/j.scriptamat.2005.10.070.

Anderson, P.M., Hirth, J.P., Lothe, J., 2017. Theory of Dislocations, 3rd ed. Cambridge University Press, Cambridge.

Arora, R., Acharya, A., 2019. Dislocation pattern formation in finite deformation crystal plasticity. Int. J. Solids Struct. doi:10.1016/j.ijsolstr.2019.02.013.

Arsenlis, A., Cai, W., Tang, M., Rhee, M., Oppelstrup, T., Hommes, G., Pierce, T.G., Bulatov, V.V., 2007. Enabling strain hardening simulations with dislocation dynamics. Model. Simul. Mater. Sci. Eng. 15, 553–595. doi:10.1088/0965-0393/15/6/001.

Bilby, B.A., Bullough, R., Gardner, L.R.T., Smith, E., 1958. Continuous distributions of dislocations IV. Single glide and plane strain. Proc. R. Soc. A 244, 538–557. doi:10.1098/rspa.1958.0059.

Bilby, B.A., Bullough, R., Smith, E., Gardner, L.R.T., Smith, E., 1955. Continuous distributions of dislocations: a new application of the methods of non-Riemannian geometry. Proc. R. Soc. A: Math. Phys. Eng. Sci. 231, 263–273. doi:10.1098/rspa.1955.0171.

Brenner, R., Beaudoin, A.J., Suquet, P., Acharya, A., 2014. Numerical implementation of static field dislocation mechanics theory for periodic media. Philos. Mag. 94, 1764–1787. doi:10.1080/14786435.2014.896081.

Cermelli, P., Gurtin, M.E., 2001. On the characterization of geometrically necessary dislocations in finite plasticity. J. Mech. Phys. Solids 49, 1539–1568. doi:10.1016/S0022-5096(00)00084-3.
de Wit, R., 1973a. Continuous distribution of disclination loops. Phys. Status Solidi 18, 669–681. doi:10.1002/pssa.2210180229.
de Wit, R., 1973b. Theory of disclinations: III. Continuous and discrete disclinations in isotropic elasticity. J. Res. Natl. Bur. Stand. – A. Phys. Chem. 77, 359–368. doi:10.6028/jres.077A.024.
Deng, J., El-Azab, A., 2010. Temporal statistics and coarse graining of dislocation ensembles. Philos. Mag. 90, 3651–3678. doi:10.1080/14786435.2010.497472.
Deng, J., El-Azab, A., 2009. Mathematical and computational modelling of correlations in dislocation dynamics. Model. Simul. Mater. Sci. Eng. 17, 075010. doi:10.1088/0965-0393/17/7/075010.
Deng, J., El-Azab, A., 2007. Dislocation pair correlations from dislocation dynamics simulations. J. Comput. Mater. Des. 14, 295–307. doi:10.1007/s10820-008-9090-4.
Devincre, B., Madec, R., Monnet, G., Queyreau, S., Gatti, R., Kubin, L., 2011. Modeling crystal plasticity with dislocation dynamics simulations: the "microMegas" code. Mech. Nano-Objects 1, 81–99. doi:10.1017/CBO9781107415324.004.
El-Azab, A., 2006. Statistical mechanics of dislocation systems. Scr. Mater. 54, 723–727. doi:10.1016/j.scriptamat.2005.11.031.
El-Azab, A., 2000. Statistical mechanics treatment of the evolution of dislocation distributions in single crystals. Phys. Rev. B 61, 11956–11966. doi:10.1103/PhysRevB.61.11956.
El-Azab, A., Po, G., 2018. Continuum dislocation dynamics: classical theory and contemporary models. In: Handbook of Materials Modeling, pp. 1–23. doi:10.1007/978-3-319-42913-7_18-1.
Gurtin, M.E., 2010. A finite-deformation, gradient theory of single-crystal plasticity with free energy dependent on the accumulation of geometrically necessary dislocations. Int. J. Plast. 26, 1073–1096. doi:10.1016/j.ijplas.2010.02.002.
Gurtin, M.E., 2006. The Burgers vector and the flow of screw and edge dislocations in finite-deformation single-crystal plasticity. J. Mech. Phys. Solids 54, 1882–1898. doi:10.1016/j.jmps.2006.03.003.
Gurtin, M.E., Anand, L., Lele, S.P., 2007. Gradient single-crystal plasticity with free energy dependent on dislocation densities. J. Mech. Phys. Solids 55, 1853–1878. doi:10.1016/j.jmps.2007.02.006.
Gurtin, M.E., Fried, E., Anand, L., 2010. The Mechanics and Thermodynamics of Continua. Cambridge University Press, Cambridge doi:10.1017/CBO9780511762956.
Gurtin, M.E., Reddy, B.D., 2016. Some issues associated with the intermediate space in single-crystal plasticity. J. Mech. Phys. Solids 95, 230–238. doi:10.1016/j.jmps.2016.05.027.
Hansen, N., Huang, X., 1998. Microstructure and flow stress of polycrystals and single crystals. Acta Mater. 46, 1827–1836. doi:10.1016/S1359-6454(97)00365-0.
Hauser, W., 1970. On the fundamental equations of electromagnetism. Am. J. Phys. 38, 80–85. doi:10.1119/1.1976233.
Hochrainer, T., 2016. Thermodynamically consistent continuum dislocation dynamics. J. Mech. Phys. Solids 88, 12–22. doi:10.1016/j.jmps.2015.12.015.
Hochrainer, T., 2013. Moving dislocations in finite plasticity: a topological approach. Z. Angew. Math. Mech. 93, 252–268. doi:10.1002/zamm.201100159.
Hochrainer, T., Sandfeld, S., Zaiser, M., Gumbsch, P., 2014. Continuum dislocation dynamics: towards a physical theory of crystal plasticity. J. Mech. Phys. Solids 63, 167–178. doi:10.1016/j.jmps.2013.09.012.
Hong, C., Huang, X., Winther, G., 2013. Dislocation content of geometrically necessary boundaries aligned with slip planes in rolled aluminium. Philos. Mag. 93, 3118–3141. doi:10.1080/14786435.2013.805270.
Huang, X., Hansen, N., 1997. Grain orientation dependence of microstructure in aluminium deformed in tension. Scr. Mater. 37, 1–7. doi:10.1016/S1359-6462(97)00072-9.
Huang, X., Winther, G., 2007. Dislocation structures. Part I. Grain orientation dependence. Philos. Mag. 87, 5189–5214. doi:10.1080/14786430701652851.
Hughes, D..A., Hansen, N., 2003. Deformation structures developing on fine scales. Philos. Mag. 83, 3871–3893. doi:10.1080/14786430310001605560.
Hughes, D...., Liu, Q., Chrzan, D.C., Hansen, N., 1997. Scaling of microstructural parameters: misorientations of deformation induced boundaries. Acta Mater. 45, 105–112. doi:10.1016/S1359-6454(96)00153-X.
Jakobsen, B., 2006. Formation and subdivision of deformation structures during plastic deformation. Science 312, 889–892. doi:10.1126/science.1124141.
Kashihara, K., Tagami, M., Inoko, F., 1996. Deformed structure and crystal orientation at deformation bands in <011> aluminum single crystals. Mater. Trans. JIM 37, 564–571. doi:10.2320/matertrans1989.37.564.
Kawasaki, Y., Takeuchi, T., 1980. Cell structures in copper single crystals deformed in the [001] and [111] axes. Scr. Metall. 14, 183–188. doi:10.1016/0036-9748(80)90091-5.
Kondo, K., 1952. On the geometrical and physical foundations of the theory of yielding. In: Proceedings of the 2nd Japan National Congress for Applied Mechanics, 2, pp. 41–47.
Kosevich, A.M.M., 1965. Dynamical Theory of Dislocations. New York 5, 579–609. https://doi.org/10.3367/UFNr.0084.196412c.0579
Kossecka, E., De Wit, R., 1977. Disclination Kinematics. Arch Mech 29.
Kröner, E., 1981. Continuum theory of defects. In: Phsique des Defauts/Physics of Defects, Les houches. North-Holland, pp. 215–315 session XXXV, 1980.
Kröner, E., 1960. General Continuum Theory of Dislocations and Proper Stresses 4, 273–334.
Kröner, E., 1959. Allgemeine kontinuumstheorie der versetzungen und eigenspannungen. Arch. Ration. Mech. Anal. 4, 273–334. doi:10.1007/BF00281393.
Kröner, E., 1958. Continuum theory of dislocations and self-stresses. Ergeb. Angew. Math. 5, 1–277.
Langdon, N., 2000. Explicit expressions for stress field of a circular dislocation loop. Theor. Appl. Fract. Mech. 33, 219–231. doi:10.1016/S0167-8442(00)00017-3.
Larson, B.C., El-Azab, A., Yang, W., Tischler, J.Z., Liu, W., Ice, G.E., 2007. Experimental characterization of the mesoscale dislocation density tensor. Philos. Mag. 87, 1327–1347. doi:10.1080/14786430600943930.
Le, G.M., Godfrey, A., Hansen, N., Liu, W., Winther, G., Huang, X., 2013. Influence of grain size in the near-micrometre regime on the deformation microstructure in aluminium. Acta Mater. 61, 7072–7086. doi:10.1016/j.actamat.2013.07.046.
Le, G.M., Godfrey, A., Hong, C.S., Huang, X., Winther, G., 2012. Orientation dependence of the deformation microstructure in compressed aluminum. Scr. Mater. 66, 359–362. doi:10.1016/j.scriptamat.2011.11.034.
Lee, E.H., 1969. Elastic-plastic deformation at finite strains. J. Appl. Mech. 36, 1. doi:10.1115/1.3564580.
Levine, L.E., Geantil, P., Larson, B.C., Tischler, J.Z., Kassner, M.E., Liu, W., Stoudt, M.R., Tavazza, F., 2011. Disordered long-range internal stresses in deformed copper and the mechanisms underlying plastic deformation. Acta Mater. 59, 5803–5811. doi:10.1016/j.actamat.2011.05.056.
Lin, F.X., Godfrey, A., Jensen, D.J., Winther, G., 2010. 3D EBSD characterization of deformation structures in commercial purity aluminum. Mater. Charact. doi:10.1016/j.matchar.2010.07.013.
Lin, P., El-Azab, A., 2019. Implementation of Annihilation and Junction Reactions in Vector Density-Based Continuum Dislocation Dynamics.
Liu, Q., Juul Jensen, D., Hansen, N., 1998. Effect of grain orientation on deformation structure in cold-rolled polycrystalline aluminium. Acta Mater. 46, 5819–5838. doi:10.1016/S1359-6454(98)00229-8.
Monavari, M., Sandfeld, S., Zaiser, M., 2016. Continuum representation of systems of dislocation lines: a general method for deriving closed-form evolution equations. J. Mech. Phys. Solids 95, 575–601. doi:10.1016/j.jmps.2016.05.009.
Morro, A., 2010. Evolution equations and thermodynamic restrictions for dissipative solids. Math. Comput. Model. doi:10.1016/j.mcm.2010.07.021.
Mura, T., 1963. Continuous distribution of moving dislocations. Philos. Mag. 24, 63–69. doi:10.1080/14786437108216424.
Nye, J.F., 1952. Some geometrical relations in dislocated crystals. Acta Metall. 1, 153–162. doi:10.1016/0001-6160(53)90054-6.
Oldroyd, J., 1950. On the formulation of rheological equations of state. Proc. R. Soc. Lond. Ser. A: Math. Phys. Sci. 200, 523–541. doi:10.1098/rspa.1950.0035.
Po, G., Huang, Y., Ghoniem, N., 2019. A continuum dislocation-based model of wedge microindentation of single crystals. Int. J. Plast. 114, 72–86. doi:10.1016/j.ijplas.2018.10.008.

Po, G., Mohamed, M.S., Crosby, T., Erel, C., El-Azab, A., Ghoniem, N., 2014. Recent progress in discrete dislocation dynamics and its applications to micro plasticity. JOM 66, 2108–2120. doi:10.1007/s11837-014-1153-2.
Reddy, J.N., 2013. An Introduction to Continuum Mechanics, 2nd ed. Cambridge University Press, Cambridge doi:10.1017/CBO9781139178952.
Reed, R.P., Clark, A.F., 1983. Materials at Low Temperatures. American Society for Metals, p. 590.
Rice, B.J.R., 1971. Inelastic Constitutive Relations for Solids: Theory and its Application 19, 433–455.
Roy, A., Acharya, A., 2006. Size effects and idealized dislocation microstructure at small scales: predictions of a phenomenological model of mesoscopic field dislocation mechanics: part II. J. Mech. Phys. Solids 54, 1711–1743. doi:10.1016/j.jmps.2006.01.012.
Sedláček, R., Schwarz, C., Kratochvíl, J., Werner, E., 2007. Continuum theory of evolving dislocation fields. Philos. Mag. 87, 1225–1260. doi:10.1080/14786430600972921.
Sills, R.B., Kuykendall, W.P., Aghaei, A., Cai, W., 2016. Fundamentals of Dislocation Dynamics Simulations. Springer Series in Materials Science, pp. 53–87. doi:10.1007/978-3-319-33480-6_2.
Steeds, J...., 1966. Dislocation arrangement in copper single crystals as a function of strain. Proc. R. Soc. Lond. Ser. A: Math. Phys. Sci. 292, 343–373. doi:10.1098/rspa.1966.0139.
Stricker, M., Sudmanns, M., Schulz, K., Hochrainer, T., Weygand, D., 2018. Dislocation multiplication in stage II deformation of fcc multi-slip single crystals. J. Mech. Phys. Solids 119, 319–333. doi:10.1016/j.jmps.2018.07.003.
Tagami, M., Kashihara, K., Okada, T., Inoko, F., 2000. Effect of cross slips on multiple slips and recrystallization in <111> and <001> Al single crystals. Nippon Kinzoku Gakkaishi/Journal Japan Inst. Met. doi:10.2320/jinstmet1952.64.7_535.
Ván, P., 2008. Objective time derivatives in nonequilibrium thermodynamics. Proc. Estonian Acad. Sci. doi:10.3176/proc.2008.3.02.
Weygand, D., Friedman, L.H., Giessen, E.Van der, Needleman, A., Van Der Giessen, E., Needleman, A., 2002. Aspects of boundary-value problem solutions with three-dimensional dislocation dynamics. Model. Simul. Mater. Sci. Eng. 10, 437–468. doi:10.1088/0965-0393/10/4/306.
Xia, S., Belak, J., El-Azab, A., 2016. The discrete-continuum connection in dislocation dynamics: I. Time coarse graining of cross slip. Model. Simul. Mater. Sci. Eng. 24, 075007. doi:10.1088/0965-0393/24/7/075007.
Xia, S., El-Azab, A., 2015a. Computational modelling of mesoscale dislocation patterning and plastic deformation of single crystals. Model. Simul. Mater. Sci. Eng. 23, 055009. doi:10.1088/0965-0393/23/5/055009.
Xia, S., El-Azab, A., 2015b. A preliminary investigation of dislocation cell structure formation in metals using continuum dislocation dynamics. IOP Conf. Ser. Mater. Sci. Eng. 89, 012053. doi:10.1088/1757-899X/89/1/012053.
Zaiser, M., Hochrainer, T., 2006. Some steps towards a continuum representation of 3D dislocation systems. Scr. Mater. 54, 717–721. doi:10.1016/j.scriptamat.2005.10.060.
Zheng, X.H., Zhang, H.W., Huang, X., Hansen, N., Lu, K., 2016. Influence of strain rate on the orientation dependence of microstructure in nickel single crystals. Philos. Mag. Lett. 96, 52–59. doi:10.1080/09500839.2016.1147653.